

MOUNTAIN-PLAINS CONSORTIUM

MPC 19-387 | J. Pace, P. Barr, and P. Powelson

Prestress Losses and
Development of Short-term
Data Acquisition System for
Bridge Monitoring



A University Transportation Center sponsored by the U.S. Department of Transportation serving the Mountain-Plains Region. Consortium members:

Colorado State University
North Dakota State University
South Dakota State University

University of Colorado Denver
University of Denver
University of Utah

Utah State University
University of Wyoming

PRESTRESS LOSSES AND DEVELOPMENT OF SHORT-TERM DATA ACQUISITION SYSTEM FOR BRIDGE MONITORING

Justin M. Pace
Paul J. Barr
Phillip Powelson

Utah State University
Department of Civil and Environmental Engineering
Logan, Utah

June 2019

Acknowledgements

This research was the result of efforts from many people beyond myself who deserve recognition for helping to bring this project to fruition.

First and foremost, I would like to thank my major professor, Dr. Paul J. Barr, for providing me with the opportunity and resources to conduct this research. Without his support, this project would never have been possible. Thank you for your time and encouragement throughout the entire research and writing process. Similarly, I would like to thank my committee members, Dr. Marc Maguire and Dr. Ziqi Song, for answering my questions, guiding this project, and being part of my education at Utah State University.

Thank you to Bridge Diagnostics, Inc. (BDI) for providing continual technical support throughout the short-term strain monitoring process. Special thanks is owed to BDI employee Rene Hamer for helping me troubleshoot the strain acquisition system multiple times throughout the year.

Other people who deserve recognition include Ethan Pickett, the graduate student who initially installed the strain data acquisition system and trained me in its use, and Piero Caputo, who helped me relocate several sensors in September. Recognition should also be given to the City of Nibley for allowing researchers to monitor its bridge and to the University Transportation Center at Utah State University for funding this project.

Finally, I would like to acknowledge the continual encouragement of my family, especially my parents, Michael and Rhonda Pace. Their support has allowed me to pursue my graduate degree at Utah State University and to be a part of this project.

Justin M. Pace

Disclaimer

The contents of this report reflect the views of the authors, who are responsible for the facts and the accuracy of the information presented. This document is disseminated under the sponsorship of the Department of Transportation, University Transportation Centers Program, in the interest of information exchange. The U.S. Government assumes no liability for the contents or use thereof.

NDSU does not discriminate in its programs and activities on the basis of age, color, gender expression/identity, genetic information, marital status, national origin, participation in lawful off-campus activity, physical or mental disability, pregnancy, public assistance status, race, religion, sex, sexual orientation, spousal relationship to current employee, or veteran status, as applicable. Direct inquiries to: Vice Provost, Title IX/ADA Coordinator, Old Main 201, 701-231-7708, ndsueoaa@ndsu.edu.

ABSTRACT

The University Transportation Center at Utah State University sponsors research through the Federal Highway Administration's University Transportation Center Program. The purpose of this research is to advance technology and expertise in transportation-related fields. This includes research on the best methods to design, monitor, and inspect bridges.

When a vehicle drives over a bridge, each bridge girder carries a portion of the vehicle's weight. This load causes strain in the bottom of the bridge girders. However, depending on where the vehicle is located on the bridge, some bridge girders carry a higher percentage of the vehicle's load. This study investigated the amount of strain typical vehicles caused in the bottom of each girder as they travel across the bridge. This research also examined the maximum strains in the bridge girders due to vehicle loads, which is of interest in girder design. In order to resist these vehicle loads, the effective prestress must be accurately determined. This project also quantified the effective prestress in an exterior and interior girder. These measured prestress forces are compared with predicted values in accordance to AASHTO LRFD specifications.

TABLE OF CONTENTS

1. INTRODUCTION.....	1
1.1 Context.....	1
1.2 Research Objectives.....	1
1.3 Organization of Paper	1
2. LITERATURE REVIEW	2
2.1 Live-Load Analysis of Posttensioned Box-Girder Bridges	2
2.2 Field Test and 3D FE Modeling of Decked Bulb-Tee Bridges.....	3
2.3 Response of Prestressed Concrete I-Girder Bridges to Live Load	3
3. SHORT-TERM STRAIN MONITORING	6
3.1 Bridge Description.....	6
3.2 Instrumentation Description.....	9
3.3 Data Collection and Processing	10
3.3.1 Data Collection	10
3.3.2 Data Processing.....	12
3.3.3 Precautions Against Data Errors	13
3.3.3.1 Drift.....	13
3.3.3.2 Multiple Event Triggers	13
3.3.3.3 Consecutive Strain Events.....	14
3.3.3.4 Noise	16
3.3.3.5 Failure to Return to At-Rest Strain Levels.....	16
3.3.4 Accuracy Verification of Results	16
3.4 Short-Term Strain Monitoring Results	18
3.4.1 Strain Summations	18
3.4.2 Distribution of Strains throughout the Day	21
3.4.3 Analysis of Large Strain Events.....	22
3.4.4 Comparison of Large Strains with Design Loading.....	25
3.4.5 Vehicle Strain Comparisons.....	27
3.4.6 Frequency Histograms	30
3.4.7 Girder Distribution Factors	37
3.5 Long-Term Prestress Losses	40
4. CONCLUSION.....	44
4.1 Summary of Conclusions.....	44
4.1.1 Summary of Conclusions for Short- and Long-Term Strain Monitoring Research	44
REFERENCES.....	45
APPENDIX A.....	46

LIST OF TABLES

Table 3.1	Largest recorded strain values for each girder.	22
Table 3.2	The 20 largest recorded strain values for all girders.	23
Table 3.3	Vehicle strain data.	28
Table 3.4	Girder distribution factors.	39

LIST OF FIGURES

Figure 2.1	Bridge 1 girder distribution factors by girder (Schwarz and Laman 2001).	4
Figure 2.2	Comparison of Bridge 2 numerical and measured GDFs for test truck runs (truck in left lane on centerline) (Schwarz and Laman 2001).	5
Figure 3.1	Photograph of the Nibley Bridge.	6
Figure 3.2	A cross-section of the Nibley Bridge at mid-span showing bridge dimensions.	7
Figure 3.3	Dimensions of a typical bridge bulb-tee girder at centerspan.	7
Figure 3.4	Plan view of the Nibley Bridge.	8
Figure 3.5	Underside of the Nibley Bridge.	9
Figure 3.6	Strain transducer attached to the bridge (Pickett 2017).	9
Figure 3.7	Initial locations of the strain transducers.	10
Figure 3.8	Adjusted locations of the strain transducers.	10
Figure 3.9	A typical strain event.	11
Figure 3.10	Screenshot of STS Monitor recording data.	11
Figure 3.11	Strain event showing the 1.0 $\mu\epsilon$ threshold as well as start and cutoff times.	12
Figure 3.12	Uncorrected and corrected drift for the same event.	13
Figure 3.13	Multiple triggers for the same strain event.	14
Figure 3.14	Consecutive strain events.	15
Figure 3.15	Strain data showing a car stopped on the Nibley Bridge.	16
Figure 3.16	Still from recorded video showing a vehicle crossing the Nibley Bridge.	17
Figure 3.17	Typical strain event for the north (left) and south (right) lanes.	18
Figure 3.18	Graph of strain magnitudes between July 30 and August 12.	19
Figure 3.19	Graph of strain magnitudes between January 14 and February 3.	20
Figure 3.20	Distribution of strains throughout the day between July 30 and August 12.	21
Figure 3.21	Distribution of strains throughout the day between January 14 and February 3.	21
Figure 3.22	Comparison of large strain events between days.	24
Figure 3.23	Largest recorded strain event.	25
Figure 3.24	Axle configuration of the International 7700 dump truck.	25
Figure 3.25	Image of the International 7700 dump truck used.	26
Figure 3.26	Strain event from a sedan.	28
Figure 3.27	Strain event from a semi-truck and trailer.	29
Figure 3.28	Strain event from a school bus.	29
Figure 3.29	Strain event from a dump truck.	30
Figure 3.30	Frequency histogram of recorded strains in Girder 1.	31

Figure 3.31	Frequency histogram of recorded strains at the bottom of Girder 2.	31
Figure 3.32	Frequency histogram of recorded strains at the centroid of Girder 2.....	32
Figure 3.33	Frequency histogram of recorded strains at the bottom of Girder 3.	32
Figure 3.34	Frequency histogram of recorded strains at the centroid of Girder 3.....	32
Figure 3.35	Frequency histogram of recorded strains in Girder 4.....	33
Figure 3.36	Frequency histogram of recorded strains in Girder 5.....	33
Figure 3.37	Frequency histogram of recorded strains in Girder 6.....	33
Figure 3.38	Frequency histogram of recorded strains in Girder 7.....	34
Figure 3.39	Frequency histogram of recorded strains in Girder 8.....	34
Figure 3.40	Frequency histogram of recorded strains in Girder 9.....	34
Figure 3.41	Frequency histogram of maximum recorded event strains in any girder.	35
Figure 3.42	Maximum bridge strains plotted on normal probability paper.	36
Figure 3.43	GVW of trucks suveyed on roads from 16 different states, annotated (Nowak and Collins 2013).	37
Figure 3.44	Girder distribution factors for north lane.	38
Figure 3.45	Girder distribution factors for south lane.	38
Figure 3.46	Girder distribution factors for multiple loaded lanes.	39
Figure 3.47	Typical girder instrumentation plan (Dimensions in mm)	40
Figure 3.48	Long-term prestressing steel strain losses at mid-span for Girder 1	41
Figure 3.49	Long-term prestressing steel strain losses at mid-span for Girder 5	41
Figure 3.50	Long-Term prestressing steel strain losses at mid-span for Girders 1 and 5	42
Figure 3.51	Mid-span stress loss comparisons	43

EXECUTIVE SUMMARY

Quantifying in-situ bridge behavior is essential for accurate design. The effects of live load are essential for bridges in general in order to understand the applied loading to the structure. For prestressed, precast concrete girder bridges, an accurate estimation of the prestress force is needed for proper design. This study's research focuses on quantifying the external loading by means of a short-term, data acquisition system, as well as quantifying the resistive prestress by monitoring the long-term changes in prestressing strand strain.

Based on the measured data, the traffic on the Nibley Bridge regularly exceeded HS-20 truck loading, with recorded strains of up to $59.26 \mu\epsilon$. The largest loading events approached (but did not exceed) the HL-93 design loads. Because the monitoring took place over a relatively narrow timespan, it was theorized that the maximum strains experienced by the bridge girders could be even higher than the measured values.

In general, the elastic shortening losses were under-predicted. This is likely due to an overestimation of the elastic modulus of the concrete. For both the interior and exterior girders, the long-term prestress losses were over-predicted by the AASHTO LRFD methods. The over-prediction of the long-term losses can be attributed to over-prediction of the creep and shrinkage losses. Overall, the long-term prestress losses for Site B and Site D were over-predicted by 31.5% and 11.1%, respectively, for the AASHTO LRFD refined method.

1. INTRODUCTION

1.1 Context

To better understand how concrete bulb-tee girder bridges respond to traffic loading, the University Transportation Center (UTC) at Utah State University sponsored research through the Federal Highway Administration UTC program. This funding is part of a regional transportation center with North Dakota State University. The goal of the research was to quantify short-term strains in concrete bulb-tee girders. The UTC also sponsored research to determine whether drone imagery could be used to create bridge models to supplement bridge inspections. The findings of both areas of this research are included in this report.

To monitor the short-term strain response of the bridge, eight strain transducers were installed on a recently constructed bulb-tee girder bridge with permission from the City of Nibley. The strain transducers were attached to the bottom of the bridge girders at mid-span. The strain transducers, datalogger, and other instrumentation were provided by Bridge Diagnostics Inc. (BDI). Data from the strain transducers were gathered over five weeks and then analyzed for patterns and trends in traffic flow.

The long-term changes in prestress were determined with embedded strain gauges, which were embedded in representative girders at the time of casting. The readings from these gauges provided changes in prestress that were compared with predictive values calculated according to the AASHTO specifications.

1.2 Research Objectives

The objective of the short-term strain monitoring area of research was to analyze the short-term strains recorded in a bulb-tee girder bridge due to everyday traffic flow. This was achieved by monitoring various bridge girders in a selected bridge. Monitoring took place over five weeks at different times of the year.

The resulting strain data were analyzed to investigate trends in both everyday traffic and extreme loading events. This included comparison of actual traffic loads to design loads and analysis of potential causes of extreme loading events. Conclusions were also drawn about the distribution of strain within the bridge girders due to everyday traffic loading. Finally, this research examined short-term loading trends and analyzed the strain caused by various vehicle types.

1.3 Organization of Paper

This paper is organized as follows:

- Section 2: Examines previous research related to girder distribution factors, load distribution in bridges, live load testing, short-term strains, drone imagery capture, and 3D modeling. Reviews details pertinent to the research conducted for this project.
- Section 3: Provides details about the monitored bridge and the instrumentation used. Discusses how strain data were collected and processed. Examines the implications of the processed strain data as they relate to this research.
- Section 4: Presents the final conclusions of this project, as well as recommendations for additional research.

2. LITERATURE REVIEW

2.1 Live-Load Analysis of Posttensioned Box-Girder Bridges

In this journal article, Hodson et al. (2012) summarize a study performed on the Lambert Road Bridge, a Type D box-girder bridge near Elk Grove, California. As part of the study, a live load test was performed on the bridge, and the results were used to validate a finite-element model (FEM) of the bridge. The FEM was then used to obtain moment distribution factors for the exterior and interior girders of the bridge. The finite-element analysis was performed while including the stiffness of bridge parapets and again without their effect. The obtained distribution factors were then compared with distribution factors calculated using procedures in the AASHTO Standard Specifications.

The researchers found that the AASHTO standard distribution factors were conservative for both the interior and exterior girders when the stiffening effects of the bridge parapets were not included. However, when the bridge parapets were included in the FEM, the distribution factors for the exterior girders were unconservative by approximately 2% to 9%. The distribution factors for the interior girders remained conservative. This finding is significant because the AASHTO LFRD specifications do not provide for the stiffening effect of parapets in distribution factors for Type D box-girder bridges. Thus, design using the AASHTO Standard Specifications for external girders is unconservative.

A parametric study was performed to investigate properties that could potentially influence the distribution factors of the bridge. The seven factors evaluated were span length, girder spacing, skew, deck overhang, continuity, deck thickness, and the thickness of the bottom girder flange. The first four parameters were accounted for in the AASHTO Standard Specifications, while the latter three were not.

Analyses were performed by incrementally changing one bridge parameter at a time in the FEM. From these analyses, it was concluded that span length and girder spacing have the greatest effect on the distribution factors. Skew and continuity had a lesser effect on the distribution factors, while deck thickness, bottom flange thickness, and deck overhang have little to no effect on distribution factors.

Based on their calculation of the FEM and parametric study, Hodson et al. proposed a new formula for the distribution factor of an external girder. This formula accounts for both span length and girder spacing and is viewable in Equation 1, where g = exterior distribution factor applied to the interior girder, d_e = horizontal distance from the centerline of the exterior web to the inside of the traffic barrier [feet (m)], S = girder spacing [feet (m)], and L = length of the span [feet (m)].

$$g = \left(\frac{(d_e + S) \cdot 0.85}{S} \right) \left(\frac{1}{L} \right)^{0.15} \quad \text{Equation 1 (Hodson et. al. 2012).}$$

Finally, the load rating of the bridge was calculated using both the distribution factors from the AASHTO LFRD specifications and from the proposed formula. The load rating from the FEM analysis was 29% higher than that obtained using the AASHTO LFRD specifications. Thus, it was concluded that the AASHTO LFRD specifications were overly conservative, and the proposed formula was recommended.

2.2 Field Test and 3D FE Modeling of Decked Bulb-Tee Bridges

In this journal article, Ma et al. (2007) summarized research on the effects of intermediate diaphragms and shear connectors on a bridge's live load distribution factors. The research also compared values for a single-lane loading condition with existing research on double-lane loaded bridges. This research focused on bridges with decked precast, prestressed concrete girders.

The study investigated four pairs of bridges. The bridge pairs represented a variety of geometries. The two bridges within each pair had similar geometries in order to allow verification of results.

Prior to testing, strain transducers were attached to the bridge at three locations: near the girders' centroid and end of span to measure shear stresses, at the bottom of the girders at mid-span to measure flexural stress, and on the intermediate diaphragms to measure axial stresses.

Two types of testing were performed on each bridge: continuous and static loading. During continuous loading, a heavily loaded dump truck was driven slowly across the bridge without stopping. During static load testing, the truck would stop at predetermined locations in order to allow changes in strains at that location to be recorded. As opposed to existing research that focused on double-lane loading, only one lane of the bridges was loaded at a time.

Using the results from the live load testing, an FE model was developed using ABAQUS software. The calibrated model was then used to determine three different live load distribution factors for a variety of bridges. Live load distribution factors were determined when a single lane of the model was loaded, when two lanes of the model were loaded, and when using AASTHO LFRD models.

The results showed that in every case the single-lane distribution factor was smaller than the double-lane distribution factor. In fact, the single-lane distribution factor was usually smaller by over 15%. Additionally, both mentioned distribution factors were typically conservative when compared with the distribution factor calculated using LRFD methods. Because the current AASHTO LRFD only allowed the one equation for both the single-lane and double-lane loading types, the researchers recommended the addition of a new equation for the single-lane loading condition.

The researchers also analyzed the effects of intermediate diaphragms and shear connectors on a bridge's live load distribution factors. It was found that the inclusion of a single diaphragm provided significant advantages over no diaphragms. However, adding additional diaphragms did not provide a notable decrease in distribution factors.

When analyzing shear connectors, researchers discovered that changing the shear connector spacing (and thus the number of shear connectors) did not have an effect on the live load distribution factors. The only difference that changing the connector spacing had was in the magnitude of vertical and horizontal forces carried by each connector. Therefore, Ma et al.'s conclusion was that if the shear connectors' capacity was adequate for the carried forces, then any number of connectors could be used without affecting the live load distribution factors.

2.3 Response of Prestressed Concrete I-Girder Bridges to Live Load

In 2001, Schwarz and Laman summarized their research on three concrete I-girder bridges. During the study, strain transducers were attached at mid-span to the bottom flange of each bridge girder. The transducers then recorded strains caused in the bridge by both normal traffic and test trucks. Research focused on three factors: dynamic load allowance (DLA), girder distribution factors (GDF), and service level stresses.

The study evaluated different factors that could potentially affect the DLA: number of axles per vehicle, vehicle speed, and span length. First, it was noted that the DLA has an inverse relationship with a bridge's maximum static stress. While the study found that the number of axles per vehicle did not have a statistically significant role in determining the DLA, it did find the DLA increased by approximately 50% when vehicle speed was increased from 45 to 55 mph (72 to 88 kph). Finally, Schwarz and Laman concluded there was no definable relationship between span length and a bridge's DLA.

Because GDFs are important factors in bridge girder design, the study also compared the measured GDFs from the live load tests with AASHTO code. GDFs were developed for both single-lane and multi-lane loading. Researchers found that among the three bridges, the measured GDF for a single lane was less than the GDF calculated using AASHTO code by at least 17%. For double-lane GDFs, the code's GDF exceeded the measured GDF by at least 22%.

The graph shown in Figure 2.1 shows the results from Bridge 1 of the study. The pair of lower, solid lines shows the measured GDFs from single-lane testing, while the dashed lines show the measured GDF ± 1 standard deviation. The upper line, "Test Trucks Side-by-Side," shows the measured GDF when a pair of trucks was driven over the bridge simultaneously. The upper line labeled "GDF₂" shows the sum of the two single-lane GDFs. Finally, the four uppermost horizontal lines show the AASHTO LFRD and AASHTO standard specifications.

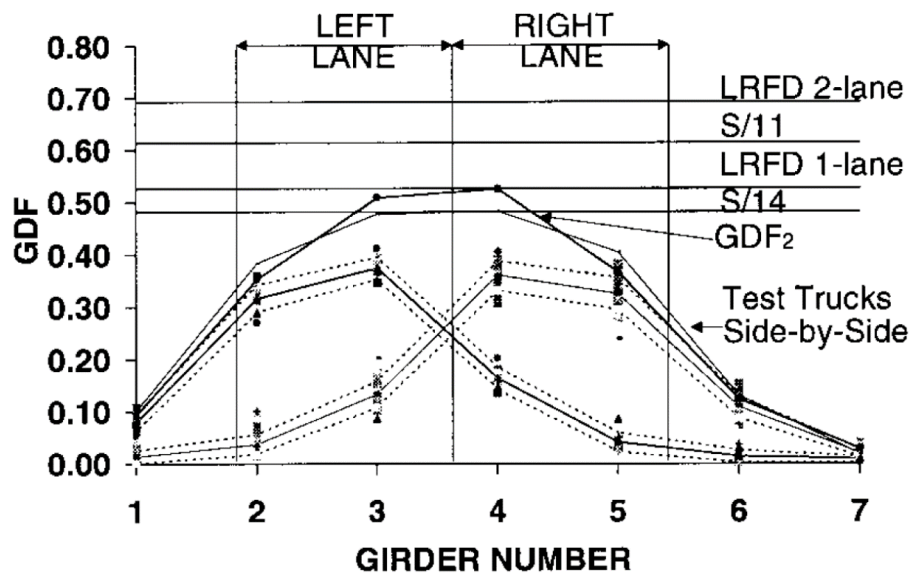


Figure 2.1 Bridge 1 girder distribution factors by girder (Schwarz and Laman 2001)

A grillage model was also developed for each bridge and compared with the live load test results. It was found that the models agreed closest with the real-world results when mid-span diaphragms were not included. As shown in Figure 2.2, the grillage models typically agreed well with the measured results. The model GDFs were typically conservative by 2% to 11%.

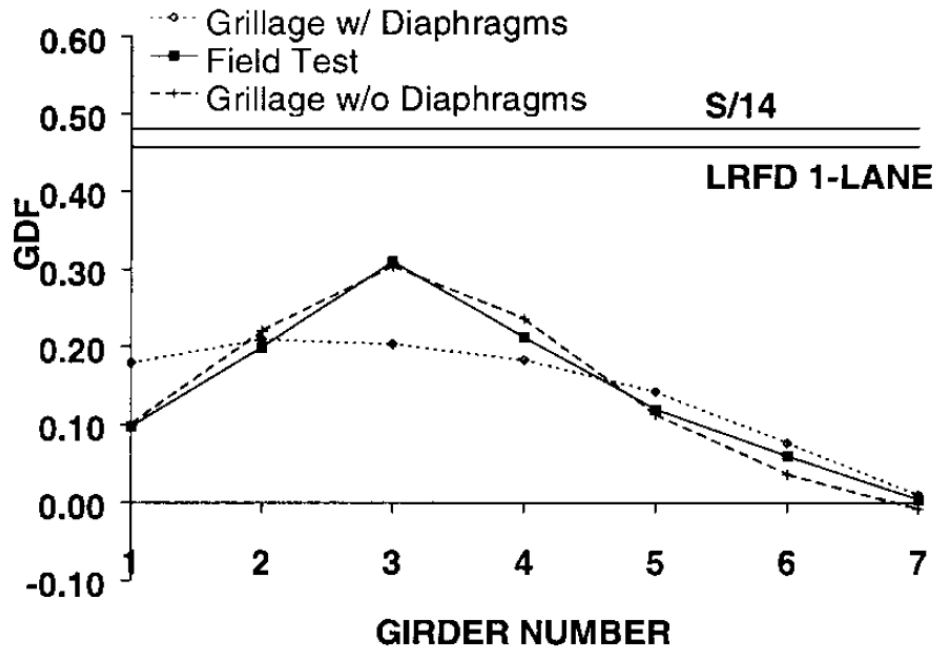


Figure 2.2 Comparison of Bridge 2 numerical and measured GDFs for test truck runs (truck in left lane on centerline) (Schwarz and Laman 2001)

From the normal traffic data, service level stresses were compiled and compared against an HS-20 truck. From these data, it was found that the interior girders directly beneath the traffic lanes had a far greater likelihood of reaching higher stresses. On Bridge 1, the girders underneath the right traffic lane experienced loading equivalent to an HS-20 truck once a day, while the remaining girders were not likely to ever reach that level of stress within the bridge's lifespan.

Schwarz and Laman reached numerous conclusions due to this study's findings. They concluded that while vehicle speed is a factor in DLAs, span length and the number of vehicle axles is not. They found that both AASHTO and modeled GDFs were conservative when compared with measured values. They also concluded that interior girders directly below the traffic lane are much more likely to see higher stress values than other girders in the bridge.

3. SHORT-TERM STRAIN MONITORING

3.1 Bridge Description

The Nibley Bridge (National Bridge Inventory Structure Number 005065F) is located in Nibley, UT. The bridge is owned by Nibley City and was designed by Forsgren Associates Inc. in conjunction with Design West Architects. The bridge is located at $41^{\circ}41'8.41''$ N and $111^{\circ}49'56.42''$ W. The bridge was designed to carry vehicle and pedestrian traffic on 2600 South across the Blacksmith Fork River to service Ridgeline High School. Figure 3.1 shows a photograph of the Nibley Bridge taken on 28 August 2017.

The Nibley Bridge was constructed from 2015-2016. Because it is the main access point for Ridgeline High School, it experiences relatively high traffic for the area depending on the time of day and season. The calculated annual daily traffic for the bridge is 1,706 vehicles/day during the school year and 1,436 vehicles/day during the summer. While the majority of vehicles crossing the bridge belong to students, parents, and school officials, there is also a relatively high volume of heavy vehicles (i.e., school buses and construction equipment) using the bridge.



Figure 3.3 Photograph of the Nibley Bridge

The bridge spans 88 feet (26.82 m) across the Blacksmith Fork River. It is 60 feet (18.28 m) wide with one 12-foot (3.66-m) lane of traffic each direction. There is also an 8-foot (2.44-m) median, two 5-foot (1.52-m) bike lanes, two 1.42-foot (0.43-m) wide parapets, and two sidewalks with a combined width of 15.17 feet (4.62 m). There is no skew or superelevation in the bridge's structure. However, the roadway itself curves slightly on top of the bridge, causing the width of the sidewalk to vary slightly along the bridge's length. Figure 3.2 shows a cross-section of the bridge at mid-span.

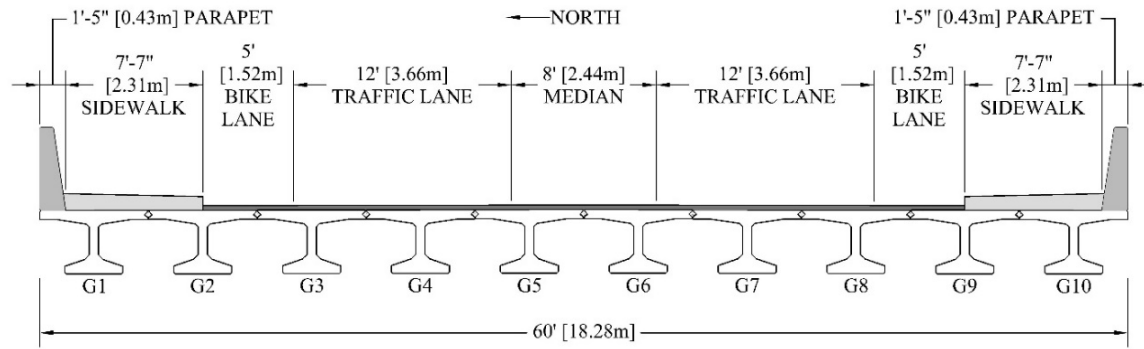


Figure 3.4 A cross-section of the Nibley Bridge at mid-span showing bridge dimensions

The 3-inch (7.62 cm) asphalt deck surface is supported by a series of 10 bulb-tee girders. Together, the girders form the deck and superstructure of the bridge. For this research, the girders were numbered G1 through G10, with G1 being the northernmost girder and G10 being the southernmost girder.

The basic girder dimensions follow that of a UDBT42 girder, with minor dimension adjustments. Every girder has the same typical cross-section, with modifications to allow tie-ins for utility pipes, barriers, etc. The dimensions of a typical girder are shown in Figure 3.3. The top of each girder contains a 2% slope to allow water to drain off the roadway.

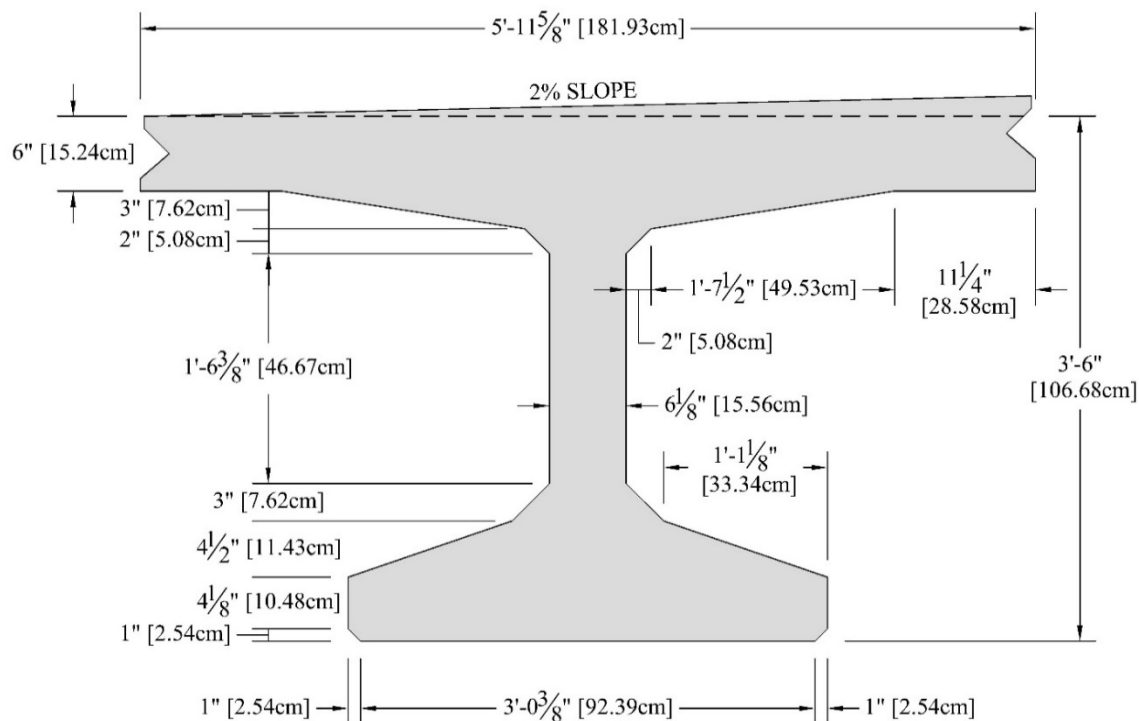


Figure 3.5 Dimensions of a typical bridge bulb-tee girder at centerspan

The girders were cast during December 2015 in Salt Lake City, Utah. The girders are prestressed longitudinally with 0.6-inch (1.52-cm) diameter AASHTO M203 Gr270 low relaxation strands. The strands have a yield strength of 270 ksi (1861.6 MPa). Ten harped strands and 24 straight strands were

used. Each prestressed strand was tensioned with a minimum force of 44 kips per strand, equivalent to 202.5 ksi (1398 MPa) stress.

The girders were designed to have an initial compressive strength (f'_{ci}) of 6.0 ksi (41.37 MPa) and a compressive strength at 28 days (f'_c) of 8.5 ksi (58.61 MPa). During casting, Girders 1 and 5 were monitored to determine actual concrete strengths. For Girder 1, f'_{ci} equaled 6.91 ksi (47.64 MPa) and f'_c equaled 10.94 ksi (75.45 MPa). For Girder 5, f'_{ci} equaled 6.72 ksi (46.33 MPa) and f'_c equaled 11.77 ksi (81.15 MPa). The girders were allowed to cure for six weeks before being transported to the bridge site. The girders were then connected longitudinally using shear connectors spaced 5 feet (1.52 m) apart.

While there is 88 feet (26.82 m) between the centerlines of the bearings, individual girders were constructed at 89.5 feet (27.28 m) long. The girders are supported on abutments that measure 91 feet (27.74 m) to the outside face and 85 feet (25.91 m) to the inside face. The abutments are 9-feet (2.74 m) tall at the exterior girders and 9.48 feet (2.89 m) along the bridge centerline. Loads are transferred from the abutments to eight 15-foot-deep (4.57 m) piles that are 12.75 inches (32.39 m) in diameter. A plan view of the bridge is given in Figure 3.4.

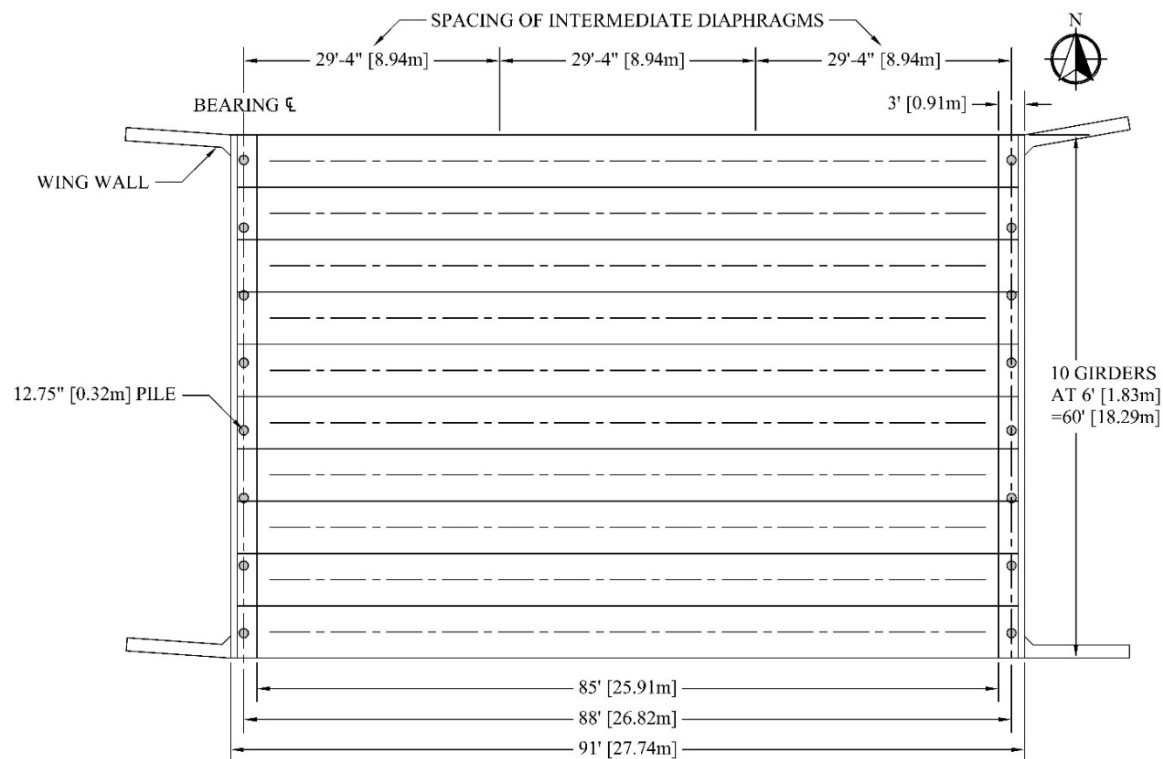


Figure 3.6 Plan view of the Nibley Bridge

Other elements of the bridge include the parapets, wing wall, and intermediate diaphragms. The parapets are on each side of the bridge and act as guardrails for pedestrians and traffic barriers for errant vehicles. The parapets are 3.5-feet (1.07-m) high and tie directly into the exterior girders. The wing walls are adjacent to the abutments on each end of the bridge and are 11.58-feet (3.53-m) tall. The wing walls extend 12 feet (3.66 m) back from the abutments and are 1.5-feet (0.46-m) thick.

Finally, two intermediate diaphragms are located at 29.33 feet (8.94 m) from each end of the bridge. The diaphragms are constructed of MC 18 x 42.7 steel channels that span between the girder webs, except for the space between Girders 3 and 4. The space between Girders 3 and 4 uses a concrete diaphragm in order to accommodate a steel pipe that runs longitudinally underneath the bridge (see Figure 3.5).



Figure 3.7 Underside of the Nibley Bridge

3.2 Instrumentation Description

For this study, the Nibley Bridge was instrumented with eight ST350 model strain transducers (See Figure 3.6). The strain transducers were attached to the exterior of the bridge using Loctite 410 adhesive and brackets. Once attached, the sensors were used to monitor the strain induced by loading the bridge. Sensors and recording equipment for this research were fabricated by Bridge Diagnostics Inc.



Figure 3.8 Strain transducer attached to the bridge (Pickett 2017)

Once attached to the bridge, the strain transducers allowed monitoring of the longitudinal strain in eight of the 10 girders. All sensors were attached at mid-span of the girders and were aligned parallel with the longitudinal axis of the girder. Strain values in unmonitored girders were assumed to have strains similar to those in monitored girders at mirrored points due to the symmetry of the bridge.

Initially, six sensors were placed at the center of the bottom flange of Girders 1 through 6, with the two additional sensors located near the centroid of Girders 1 and 2 (See Figure 3.7). Upon review of the data, the two sensors located at the neutral axis (B1987 and B1979) were recording values near zero. The gauge located at the bottom of Girder 1 also recorded near-zero strains. It was decided to move these three sensors to maximize the study. In September 2017, the sensors attached to the girder centroids and to the bottom of Girder 1 were moved to the center of the bottom flange of Girders 7, 8, and 9 in order to monitor those girders as well (See Figure 3.8).

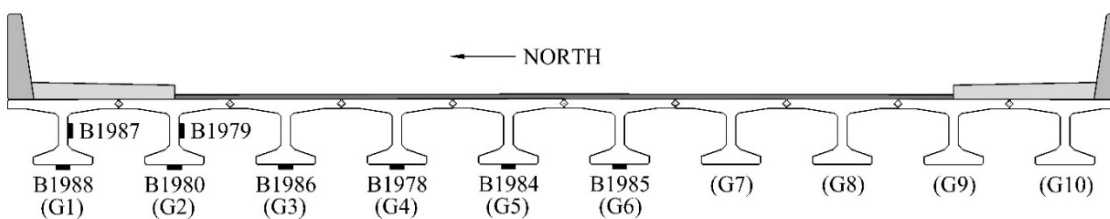


Figure 3.9 Initial locations of the strain transducers

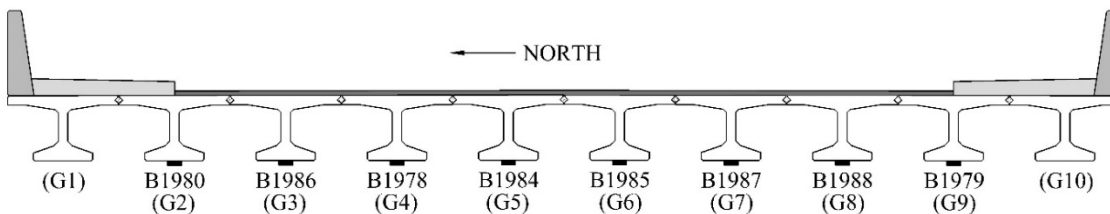


Figure 3.10 Adjusted locations of the strain transducers

3.3 Data Collection and Processing

3.3.1 Data Collection

Once the strain transducers were attached to the bridge, traffic over the bridge was monitored over several weeks. Because much of the bridge traffic is destined for the nearby high school, data were recorded during both the summer (July 29-August 11) and the winter (January 7-January 27) in order to determine strain levels while school was both in and out of session.

This research focused on strain “events.” Each loading event was characterized by a noticeable increase in strain, followed by a return in strain to near at-rest levels (i.e., approximately $0 \mu\epsilon$) (See Figure 3.9). Positive strain values corresponded to tension in the girder.

Typically, events were caused by traffic driving over the bridge. As a vehicle drove over the bridge, the strain at the bottom of each girder would increase until the vehicle was positioned to cause the maximum moment in the girders. It would then decrease as the vehicle drove off the bridge, at which point the strains returned to measure at-rest levels.

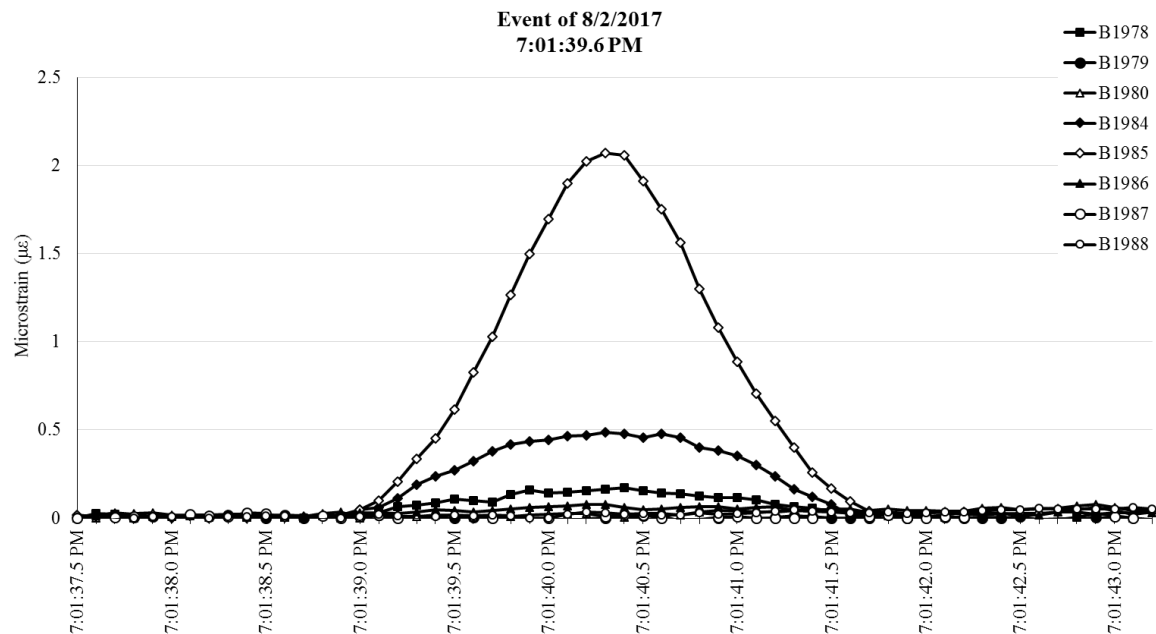


Figure 3.11 A typical strain event

Data were recorded using Bridge Diagnostics Inc.'s STS Monitor software (Figure 3.10). While the STS Monitor software has the ability to record individual strain events, it was discovered that the software failed to record all of the strain events that occurred on the bridge. Instead, the STS Monitor software was set to continuously capture strain data from each sensor every 0.1 seconds. These data were recorded in technical data management streaming (TDMS) files that were saved to the datalogger. An add-in allowed the TDMS files to be opened and manipulated in Microsoft Excel.



Figure 3.12 Screenshot of STS Monitor recording data

3.3.2 Data Processing

The focus of the research called for the examination of individual strain events; however, the TDMS files were recorded as four-hour-long blocks of continuous data. To avoid combing through hundreds of hours of data to manually identify strain events, two programs were written in Visual Basic for Applications (VBA) that would extract data about individual strain events and then compile the strain data into a consolidated Excel workbook.

The first VBA program identified sections in the continuous data where one or more sensors suddenly experienced a rapid increase in strain. The program identified rapid increases in strain by finding the value of each data point minus the minimum strain value from the previous 6.0 seconds for each sensor. If the difference between the two values was greater than $1.0 \mu\epsilon$, the program would copy all of the strain data from 3.0 seconds before the rise in strain began to 3.0 seconds after the strain values began to lower to at-rest values (See Figure 3.11). It will also copy the 6.0-second minimum data. Finally, the VBA program would paste the copied information into a separate Excel workbook, save it, and continue scanning the TDMS files for further events.

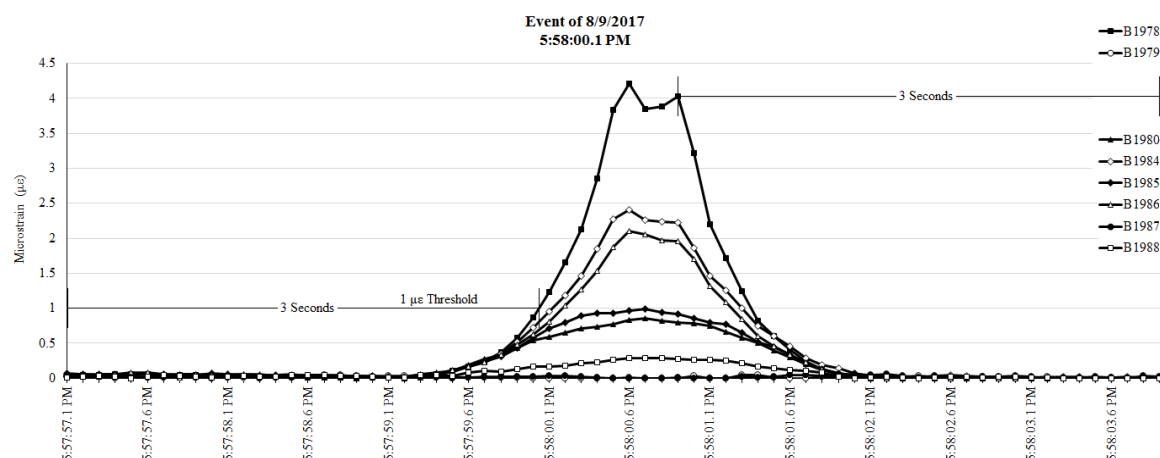


Figure 3.13 Strain event showing the $1.0 \mu\epsilon$ threshold as well as start and cutoff times

Strain events that never crossed the $1.0 \mu\epsilon$ threshold were considered negligible and ignored by the event extraction program. A $1.0 \mu\epsilon$ threshold was chosen after higher thresholds were shown to exclude a percentage of light motor vehicles. A trial-and-error approach was used to determine that the majority of vehicles caused greater than $1.0 \mu\epsilon$ in bridge girders.

Once each strain event had been extracted into its own Excel workbook, the second VBA program would open the workbook for each event, read the maximum strain values for every sensor, and compile the maximum strain data values into a consolidated Excel workbook. The comprehensive workbook was then used as a basis for the conclusions found in Section 3.4. Copies of both of the VBA programs can be found in Appendix A.

It is important to note that not every vehicle produced a strain event. For example, pedestrians, bicycles, motorcycles, and other light loading might produce a strain event below the $1.0 \mu\epsilon$ threshold. Likewise, some vehicles might produce more than one strain event. It was observed that semis hauling multiple trailers could have multiple, separate events. Finally, if two vehicles were on the bridge at the same time (either in separate lanes or one behind another) and strain levels did not return to a near-zero level between the two events, the combined response of the two vehicles would create a single strain event.

3.3.3 Precautions Against Data Errors

Several safeguards were implemented to make certain that the VBA programs accurately read and extracted the event data. These safeguards included precautions against drift, counting the same event twice, consecutive strain events, noise, and failure to return to at-rest strain levels. To minimize the effect that these potential errors had on the results, sections of code were included in the two programs to address each problem.

3.3.3.1 Drift

Because the BDI sensors were initially intended for short-term recording, they experienced a certain amount of drift throughout the day. The STS Monitoring software was designed to zero out the strain in the sensors when recording began. As the time passes, changes in temperature and other environmental factors can cause the at-rest value of strain in the sensors to vary, even when there is no applied load on the bridge. For example, sensors that began by recording 0 $\mu\epsilon$ in the morning might be reading 30 $\mu\epsilon$ in the heat of the day and -20 $\mu\epsilon$ at night.

To compensate for drift, the strain compilation program would subtract the 6.0-second minimum value from the maximum strain value recorded by each sensor. This would transform the event on the left in Figure 3.12 to the event on the right. The VBA program would then copy the adjusted maximum value to the consolidated workbook as the maximum event strain.

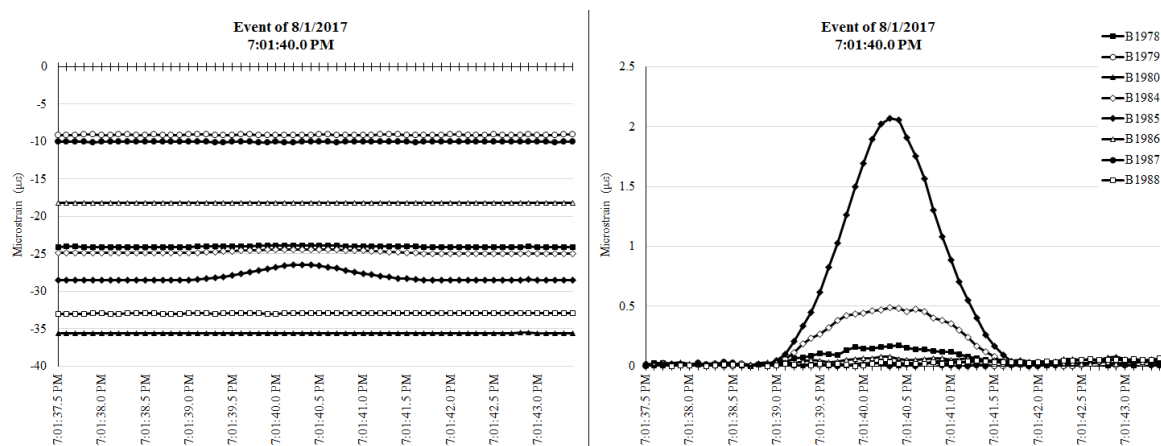


Figure 3.14 Uncorrected and corrected drift for the same event

3.3.3.2 Multiple Event Triggers

In several cases, the same strain event would have multiple points that could trigger the program to copy it to a new workbook. For example, every point in the shaded area in Figure 3.13 could independently trigger the event extraction program to create a separate event. This would result in 19 separate Excel files of the same event.

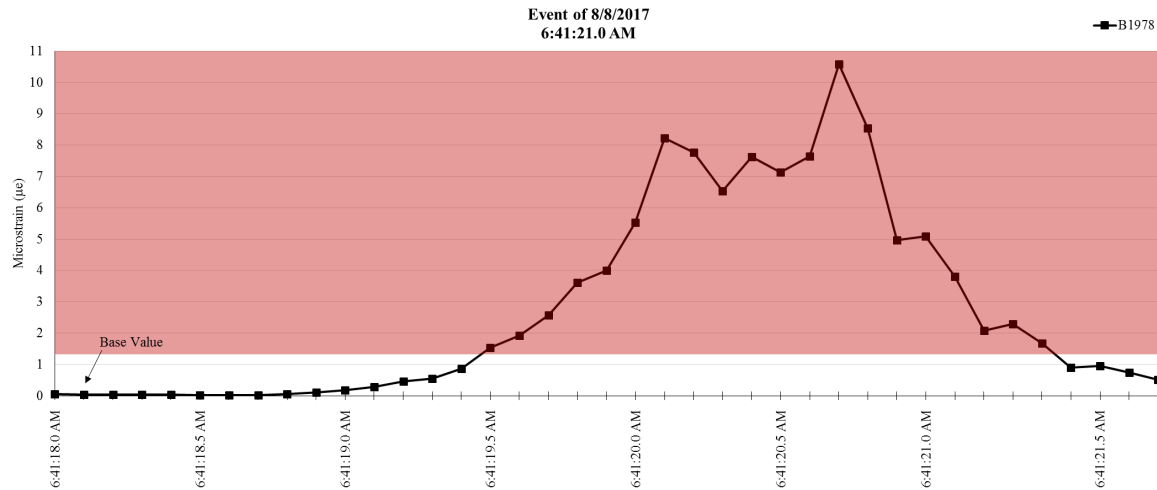


Figure 3.15 Multiple triggers for the same strain event

In order to force the program to create only one workbook for each event, a segment of code was used that forced the program to ignore additional event triggers for 0.5 seconds after an event had begun. A 0.5-second window was chosen because, for a vehicle to cross the bridge in one second, it would be traveling 140.4 mph (113.0 kph) in a 25 mph (40.2 kph) speed zone. Therefore, a vehicle is unlikely to cross the entire bridge (i.e., create a complete strain event) in a single second. Any additional vehicles coming onto the bridge during the one-second window would end up contributing to the original event instead of creating a new, separate event.

Additionally, if an event had been triggered within the previous 10 seconds, the program checked whether the program was a large strain event. It did so by subtracting a base value from the strain value that created the new trigger. The program would then check to see whether the difference was reasonably close to the 1.0 µε threshold. If not, the new trigger was ignored (i.e., for the event shown in Figure 3.13, the event is initially triggered at 6:41:19.6 AM. One second later, the strain is at 7.64 µε, which is not reasonably close to 1.0 µε, so the program determines it is a large strain event and ignores the additional trigger).

3.3.3.3 Consecutive Strain Events

Occasionally, multiple vehicles drove over the bridge within a matter of seconds of each other. When this happened, it was challenging for the event extraction program to count the number of vehicles accurately. The event extraction and strain compilation programs were designed to work best when single vehicles drove over the bridge one at a time.

To demonstrate some of the issues involved with consecutive strain events, Figure 3.14 shows an example of when two vehicles crossed the bridge within a few seconds of each other. Each vehicle created its own event file, but each event file contained information from both events. The first vehicle's event file spanned Point A to Point D, while the second vehicle's event file spanned Point B to Point E.

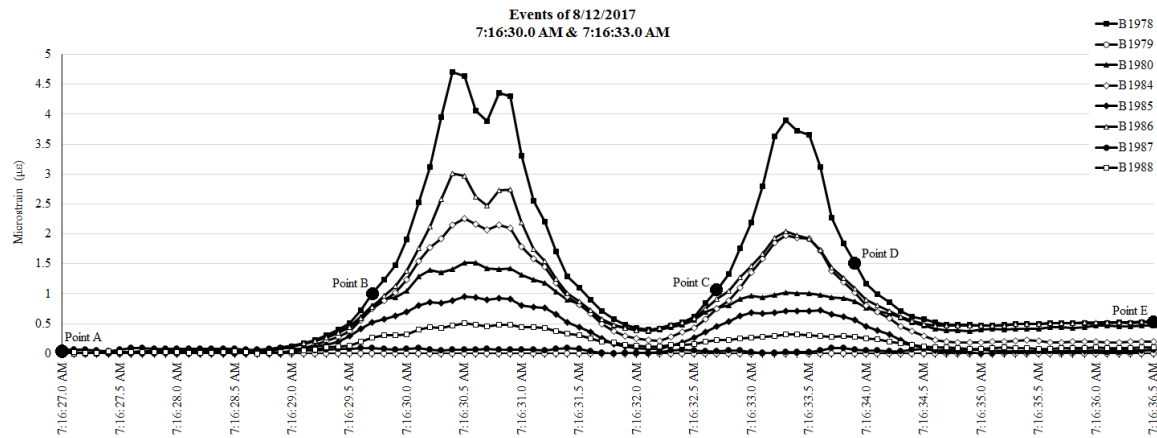


Figure 3.16 Consecutive strain events

The above scenario created several problems. The event extraction program originally detected events by comparing each data point against the data point exactly 3.0 seconds before it. For the second event in Figure 3.14, this was the difference between Point C and Point B. Because the difference between these two points is only $0.06 \mu\epsilon$, the original event extraction program would not have detected the second event. To address this, the program was modified to subtract the minimum value from the last 6.0 seconds from Point C instead (a difference of $1.07 \mu\epsilon$).

Currently, the strain compilation program calculates the maximum strain in each file by subtracting the 6.0-second minimum from the maximum strain. Initially, the strain compilation program took the maximum strain value from anywhere in the event file. This caused inaccurate readings, because when it read the file for the second strain event file (comprising points between Point B and Point E), the program detected the maximum from the first strain event instead.

This issue was addressed by modifying the program to take the maximum strain value after the $1.0 \mu\epsilon$ threshold was crossed (the second event crosses the threshold at Point C). However, if the second event was larger than the first, the program could still use the maximum strain from the second event when calculating the maximum strain of the first event (which contains data from Point A to Point D). This remains a known issue with the strain compilation program.

If a vehicle stopped on the bridge, it also created problems. For example, in Figure 3.15, a car stopped on the bridge to pick up pedestrians. Then, at 2:44:28 pm, a second car crossed the bridge. Because the strain compilation program only considers data from up to six seconds before the start of the event, the maximum strain for the second vehicle stopped did not include the initial strain caused by the stopped vehicle. Instead, it only included the additional strain caused by the second vehicle driving onto the bridge. The strain compilation program faced similar problems if heavy traffic at the nearby stoplight caused vehicles to back up onto the bridge.

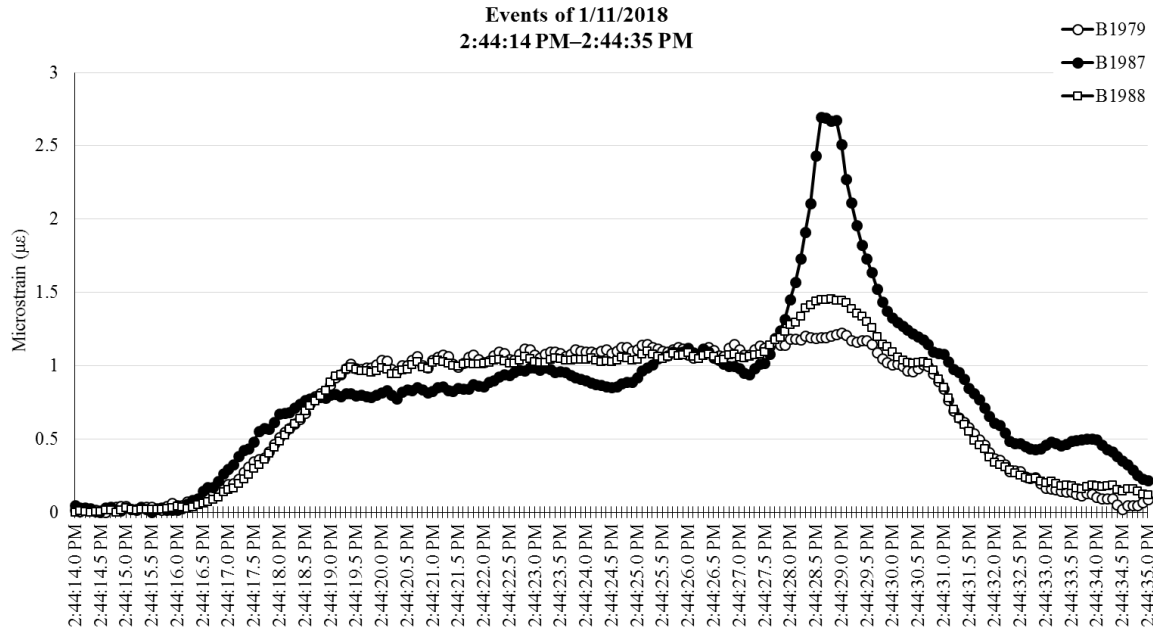


Figure 3.17 Strain data showing a car stopped on the Nibley Bridge

3.3.3.4 Noise

All sensors experience a level of variation in their data called noise. Testing the BDI sensors revealed that the strain transducers experienced variation between 0.01 and 0.15 $\mu\epsilon$ while the bridge was unloaded. In order to avoid picking up sensor noise as actual strain events, a 1.0 $\mu\epsilon$ trigger threshold was selected for this project. It was observed that the majority of vehicles caused a strain greater than 1.0 $\mu\epsilon$. Any sudden increases in strain that did not exceed 1.0 $\mu\epsilon$ were ignored by the event extraction program. Setting the threshold at 1.0 $\mu\epsilon$ also helped combat drift, which could trigger a false event if the threshold was set lower.

3.3.3.5 Failure to Return to At-Rest Strain Levels

Occasionally, the program would fail to return to normal strain levels at the end of the event. While the exact cause for this is unknown, it could potentially be related to vehicles parking on the bridge. When the program did not return to at-rest levels of strain, the event extraction program was set to extract a maximum of 30 seconds of data. This prevented a single event file from lasting for several minutes and containing multiple events.

3.3.4 Accuracy Verification of Results

To ascertain that the developed event extraction program could accurately locate and extract the strain events caused by traffic, video monitoring was set up at the Nibley Bridge (See Figure 3.16). The selected video camera, GoPro Hero5 Black, recorded vehicles driving over the bridge over the period of an hour. The footage of the traffic was then reviewed and compared against processed strain data for the same time period for validation purposes.



Figure 3.18 Still from recorded video showing a vehicle crossing the Nibley Bridge

Video was recorded between 2:00 and 3:00 P.M. on 11 January 2018. This time was chosen because it allowed for video capture during two different traffic flow levels. During most of the day, traffic on the bridge is comparatively low. The exception is just before school starts at 8:00 A.M. and right after school lets out at 2:45 P.M., when for a brief period the traffic volume is comparatively high. For the purposes of comparison, data were analyzed separately from 2:00 to 2:30 P.M. and from 2:30 to 3:00 P.M.

Between 2:00 and 2:30 P.M., the video recording showed 71 vehicles crossed the Nibley Bridge. The event extraction program was able to detect and extract 67 events. The four omitted events involved vehicles in opposite lanes crossing the bridge within 0.5 seconds of each other; per the definition of a strain event in Section 3.3.2, the strains caused by these vehicles were treated as a single strain event. Under these conditions, 94.4% of vehicles triggered strain events, and 100% of vehicle strain data were accurately extracted.

Between 2:30 and 3:00 P.M., 311 vehicles crossed the Nibley Bridge. The event extraction program was able to detect and extract 261 strain events. The program also extracted a single event twice due to an exceptionally high amount of noise that coincided with the event. Due to the high traffic volume, the specific causes of each omitted event could not be determined. However, the event extraction program was successfully able to detect and extract strain data files for 83.7% of vehicles.

At approximately 2:48 P.M., the traffic volume was so high that traffic backed up on the bridge in the north lane for approximately 1.7 minutes. Because the event extraction program only extracts data from the previous six seconds, the strain compilation program only considered additional strain caused by new vehicles driving onto the bridge, not the total strain in the bridge girders, during this window. Additionally, most vehicles followed each other so closely that the heaviest vehicles (i.e., school buses) appeared in multiple events; the strains caused by the heaviest vehicles were counted multiple times by the strain compilation program.

Comparing the event extraction program against the bridge traffic video footage demonstrates that the event extraction program can accurately detect and extract events from the raw TDMS files. While the program had difficulty distinguishing between vehicles during levels of high traffic, it was still able to extract events for 83.7% of all vehicles. During periods of low traffic, the program was able to extract 100% of vehicle strain data. Because the bridge experiences high volume of traffic for no more than 5% of the day, the event extraction and strain compilation programs were deemed adequate for the purposes of this research.

Finally, because strain events with exceptionally high levels of strain were of the greatest interest to this research, every high-level strain event recorded over the five weeks of monitoring was hand-checked prior to drawing the conclusions in Section 3.4. This was done by opening the individual file for each event and plotting a graph of strain over time to verify that the maximum strains had been accurately extracted. If necessary, the raw, continuous TDMS file was consulted to give context to the data.

3.4 Short-Term Strain Monitoring Results

3.4.1 Strain Summations

It was discovered that Girders 4 (Sensor B1978) and 7 (Sensor B1987) experienced the highest strains. These girders regularly experienced strains 185% to 250% higher than strains in adjacent girders. As the magnitude of the strains in Girders 4 and 7 increased, the difference in strains between adjacent girders also increased.

Girders 3 (Sensor B1985), 5 (Sensor 1984), 6 (Sensor B1985), and 8 (Girder 1988) experienced the second-highest strains. Each of Girders 3-8 is directly beneath the traffic lanes. The lowest strains at the bottom of a girder were recorded when Sensor B1988 was placed beneath Girder 1, an exterior girder. When the sensors were placed at the neutral axis of the girders, they experienced little to no strains. Figure 3.17 shows a typical strain event for a single vehicle in the north (left) and south (right) lanes.

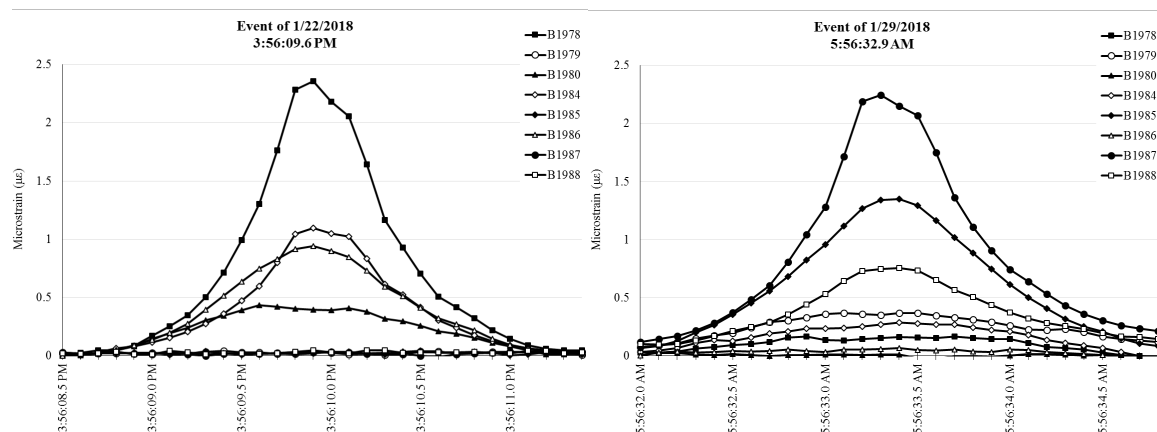


Figure 3.19 Typical strain event for the north (left) and south (right) lanes

Between January 14 and February 3 (three weeks), the strain transducers recorded 35,843 events. In the two-week period from July 30 to August 12, the strain transducers recorded 19,053 events. However, during the summer, Girder 7 was not monitored, which meant that several vehicles likely crossed the Nibley Bridge in the south lane without triggering an event.

Analyzing the wintertime data shows that 9.0% of events recorded in the south lane did not trigger an event in Girder 6 (the only south-lane girder monitored during the summer). Assuming this ratio is constant year-round suggests that an additional 1,052 events in the south lane were not recorded by the datalogger during the summer. This gives an estimated 20,105 total events during the summer recording period.

Graphs showing the magnitude of the recorded strains are shown in Figure 3.18 (summer) and Figure 3.19 (winter). Both figures show the largest strain recorded by any sensor for each event. Each figure subdivides the recorded strains into individual weeks.

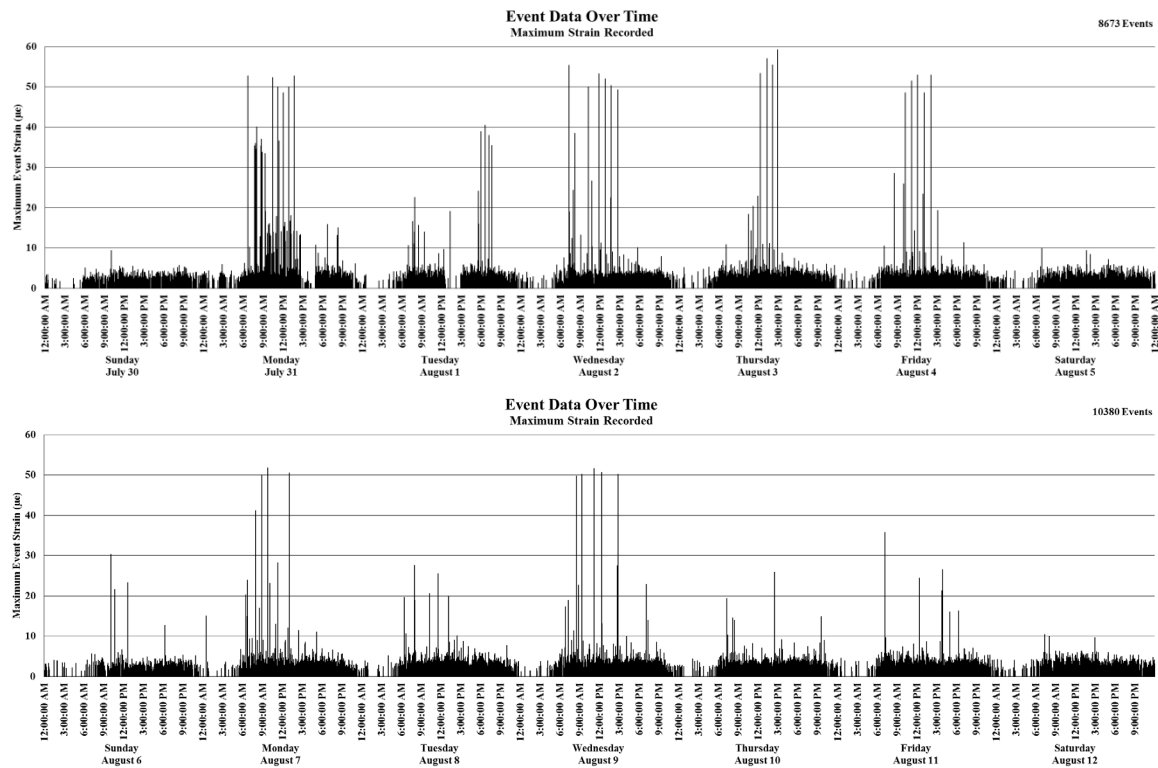


Figure 3.20 Graph of strain magnitudes between July 30 and August 12

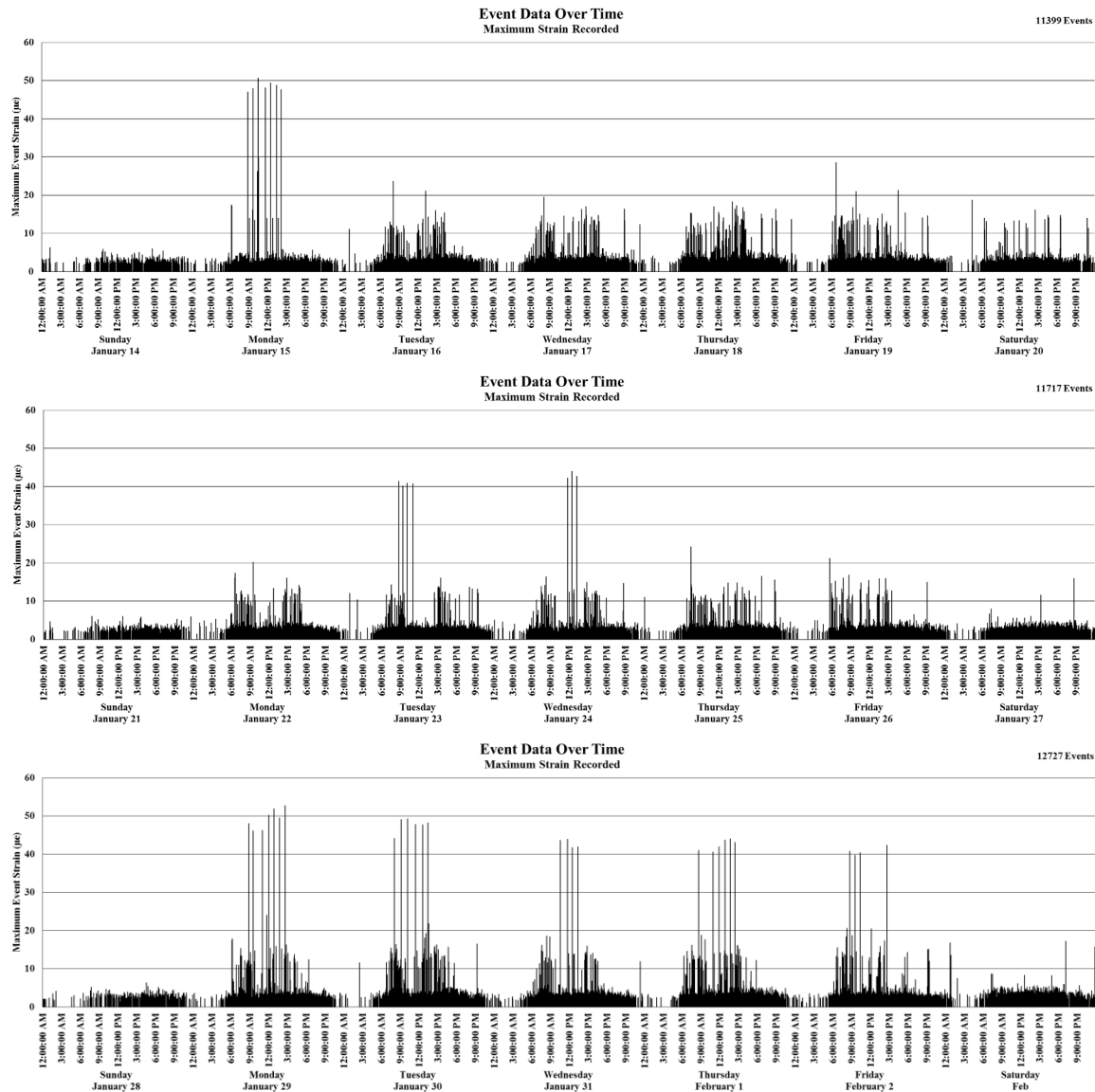


Figure 3.21 Graph of strain magnitudes between January 14 and February 3

Figures 3.18 and 3.19 show the traffic flow is relatively consistent throughout the day and the majority of strains do not exceed $5.0 \mu\epsilon$. Traffic flow decreases at night, with comparatively little traffic between midnight and 5:00 A.M. There was a noticeable rise in strains in the $10\text{--}20 \mu\epsilon$ range during the winter, which is attributable to additional school buses crossing the bridge (note that in Figure 3.19 there are clusters of strain in the $10\text{--}20 \mu\epsilon$ range when buses would be arriving at and leaving the school). There are also several strains significantly higher than the rest, and these will be discussed further below.

During the summer, the Nibley Bridge had annual average daily traffic of 1,436 vehicles/day. During the winter, the bridge had annual average daily traffic of 1,706 vehicles/day. This corresponds to an 18.85% increase in traffic while school is in session.

The majority of events were observed to last about 3.25 seconds. This appears reasonable, as it corresponds to a vehicle speed of 22.6 mph (26.4 kph). The speed limit on the bridge is 25 mph (40.2 kph). However, some events lasted as long as 13 seconds. These events mostly correspond with larger vehicles accelerating after turning off the nearby intersection or roundabout.

3.4.2 Distribution of Strains throughout the Day

Further analysis of Figures 3.18 and 3.19 resulted in Figures 3.20 and 3.21. These figures show the distribution of strains throughout the day, regardless of their magnitude. During the summer, traffic flow was relatively consistent throughout the day and corresponded with anticipated trends relating to traffic patterns. For example, the largest percentage of traffic occurred between 5:00 P.M. and 6:00 P.M., which corresponds to employees returning home from work.

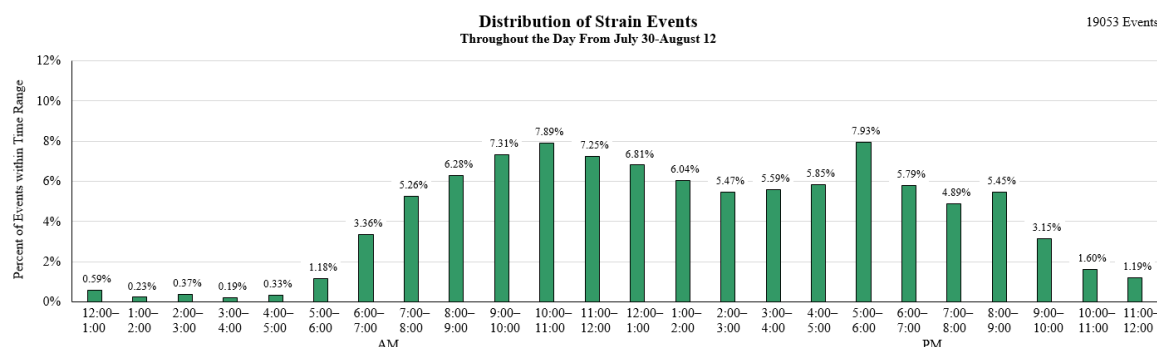


Figure 3.22 Distribution of strains throughout the day between July 30 and August 12

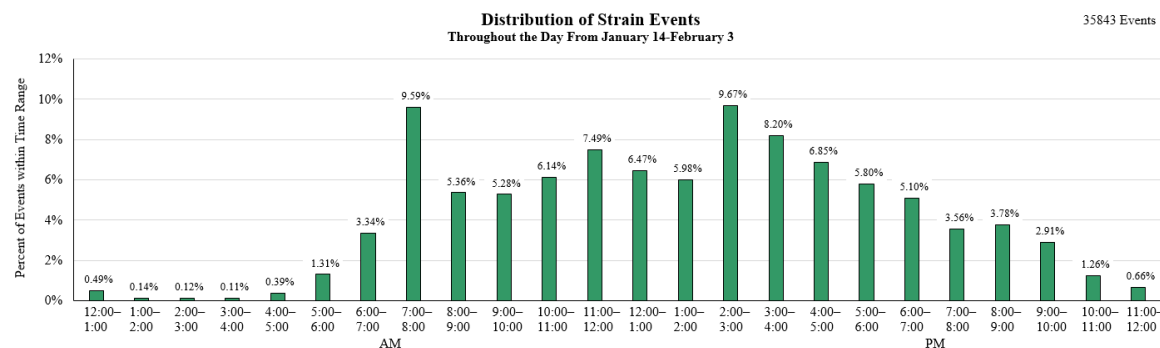


Figure 3.23 Distribution of strains throughout the day between January 14 and February 3

During the winter, the highest traffic volumes corresponded with school beginning at 8:00 A.M. and letting out at 2:45 P.M. On days when school was in session, an average of 480 vehicles crossed the bridge in the half hour before school started (7.69% of the day's traffic). An average of 469 vehicles crossed the bridge within half an hour of school letting out (7.50% of the day's traffic). From these data, it can be concluded that traffic flow was more concentrated while school was in session, resulting in multiple vehicles using the bridge at once and larger strains in the bridge girders.

3.4.3 Analysis of Large Strain Events

Figures 3.18 and 3.19 also reveal that several large vehicles crossed the bridge on a semi-regular basis. Table 3.1 shows the largest strain values recorded for each girder for both monitoring periods.

Table 3.1 Largest recorded strain values for each girder

Largest Recorded Strain ($\mu\epsilon$)	Girder Number & Associated Sensor									
	1	2	3	4	5	6	7	8	9	10
	B1988	B1980	B1986	B1978	B1984	B1985	B1987	B1988	B1979	N/A
Summer	7.24	18.55	30.87	59.26	40.46	40.46	N/A	N/A	N/A	N/A
Winter	N/A	15.94	28.22	52.78	26.70	20.35	26.31	13.66	10.72	N/A
Overall	7.24	18.55	30.87	59.26	40.46	40.46	26.31	13.66	10.72	N/A

While the largest values recorded in Table 3.1 tend to not vary significantly between the summer and winter, larger strains occurred during the summer in every monitored girder. This is likely due to the increased use of heavy construction equipment during the summer months.

Table 3.1 also shows that, to an extent, the assumption of symmetry in strains between girders is valid. The largest exception to this assumption is Girders 4 and 7. When these two girders were monitored simultaneously during the winter, the difference between the recorded maximums was 26.47 $\mu\epsilon$. Potential reasons why the strains in Girder 4 are so much higher are discussed further below.

While Table 3.1 tabulates the largest strain value seen in each girder, Table 3.2 presents the largest 20 strain values caused in any girder. Each strain value has been checked for accuracy by plotting a graph of the event to see if it appeared accurate. It is important to note that every strain in Table 3.2 occurred in Girder 4 (Sensor B1978).

Table 3.2 The 20 largest recorded strain values for all girders

Time of Vehicle Crossing	Microstrain Caused by Vehicle
3 Aug 2017 — 2:47:58 PM	59.26 $\mu\epsilon$
3 Aug 2017 — 1:15:25 PM	57.01 $\mu\epsilon$
3 Aug 2017 — 2:02:33 PM	55.42 $\mu\epsilon$
2 Aug 2017 — 7:15:42 AM	55.31 $\mu\epsilon$
3 Aug 2017 — 12:12:32 PM	53.38 $\mu\epsilon$
2 Aug 2017 — 11:46:29 AM	53.30 $\mu\epsilon$
4 Aug 2017 — 11:59:41 AM	52.98 $\mu\epsilon$
4 Aug 2017 — 2:03:47 PM	52.91 $\mu\epsilon$
29 Jan 2018 — 2:38:59 PM	52.78 $\mu\epsilon$
31 Jul 2017 — 6:40:37 AM	52.78 $\mu\epsilon$
31 Jul 2017 — 1:40:55 PM	52.76 $\mu\epsilon$
31 Jul 2017 — 10:23:31 AM	52.27 $\mu\epsilon$
2 Aug 2017 — 12:43:30 PM	51.96 $\mu\epsilon$
29 Jan 2018 — 12:51:29 PM	51.89 $\mu\epsilon$
7 Aug 2017 — 9:48:30 AM	51.78 $\mu\epsilon$
9 Aug 2017 — 11:07:16 AM	51.57 $\mu\epsilon$
4 Aug 2017 — 11:07:10 AM	51.50 $\mu\epsilon$
15 Jan 2018 — 10:29:46 AM	50.66 $\mu\epsilon$
9 Aug 2017 — 12:17:55 PM	50.62 $\mu\epsilon$
7 Aug 2017 — 1:01:39 PM	50.52 $\mu\epsilon$

Because Girder 4 falls directly underneath the north lane, it experiences the largest strains of any girder due to westbound traffic. However, its strains are exceedingly bigger than the largest strains in the corresponding south-lane girder. Four possible explanations are presented as to why Girder 4 experienced larger strains than other girders.

First, the strain transducer attached to Girder 4 (Sensor B1978) could need calibration. However, we know that Girder 7, the corresponding girder in the south lane, regularly experiences strains 185% to 250% higher than strains in its neighboring girders. This ratio is similar for the north lane as well, suggesting that Sensor B1978's readings may be correct.

Second, the traffic light to the west of the bridge provides vehicles an easy way to turn south onto Utah State Road 165. Because UT-165 has a posted speed limit of 55 mph (88.51 kph), large vehicles turning left need to use a traffic signal to give them time to make the turn and accelerate. The traffic light near the Nibley Bridge is the only signal for 1.19 miles (1.92 km) to the north and 0.75 miles (1.20 km) to the south. Because the Utah Department of Transportation is currently doing roadwork on UT-165 to the south of Ridgeline High School, there are multiple construction vehicles that use this intersection to turn south onto UT-165. Vehicles turning south would cross the north lane of the bridge, but not the south lane.

Third, the girders in the south lane may have a better joint connection than the girders in the north lane. If so, Girder 7 would distribute more load into its neighboring girders than Girder 4, resulting in higher comparative strains in Girder 4. A difference in the degree of composite behavior could potentially be caused by discrepancies in the way the girders were installed or damage in the connectors by excessive loading.

Fourth, trucks could be retrieving material from an area east of the bridge and transporting it to an area west of the bridge. If this is true, trucks crossing the bridge would be heavier when they cross the north lane, and lighter when they return using the south lane.

Referring to Figures 3.18 and 3.19 shows that multiple large events often occurred in a single day. On other days, there were few, if any, large events. Reviewing Table 3.2 shows that many events with similar magnitudes of strain occurred on the same day. Because of this, it is likely that the largest strains for each day were caused by the same vehicle.

This conclusion is supported by Figure 3.22, which plots two large events from July 31, 2017 (left), against two large events from January 29, 2018 (right). Even though the events on both sides produced similar magnitudes of strain in the bridge, they appear drastically different. Note that the two events shown for August 3 are similar in both shape and the time it took to cross the bridge, suggesting they were caused by the same vehicle. The same applies to the two events from January 31. Incidentally, the vehicle on the left likely had four axles (because there are four peaks within the event), while the vehicle on the right likely only had two axles.

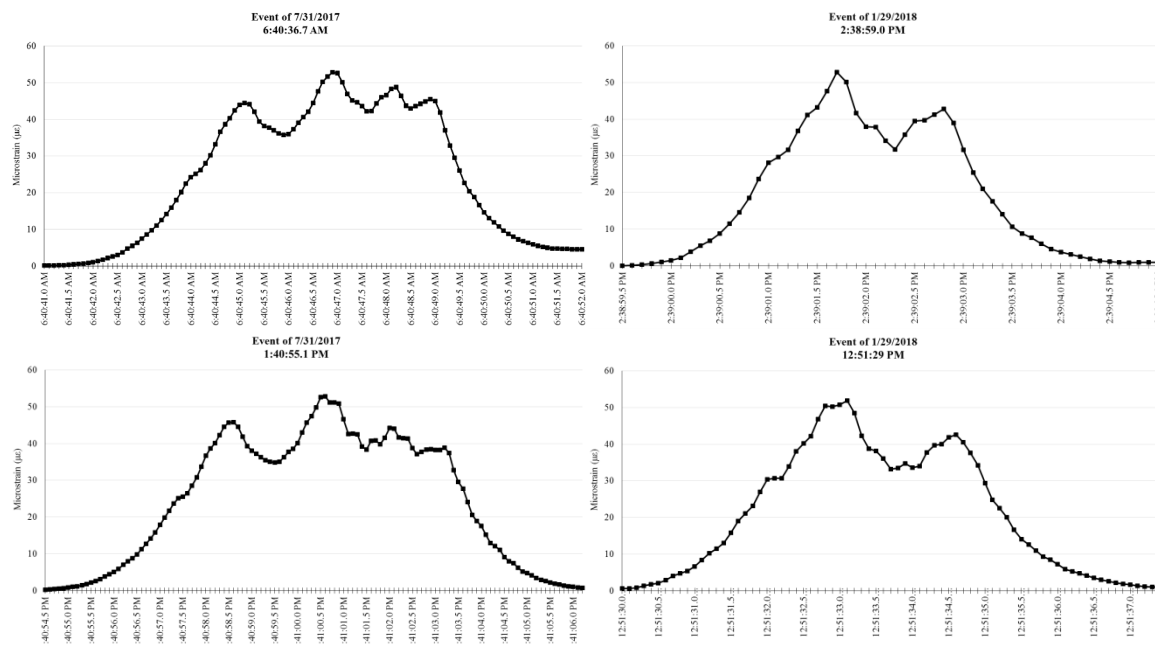


Figure 3.24 Comparison of large strain events between days

The largest recorded strain event occurred at 2:47:58 P.M. on August 3, 2017 (see Figure 3.23). The vehicle took 8.3 seconds to cross the bridge and caused a strain of 59.26 $\mu\epsilon$. While the exact type of vehicle that caused this strain event is unknown, analysis of Figure 3.23 shows it was likely a double trailer dump truck with six axles crossing the north lane. Given the magnitude of strain it caused, it would have been carrying a heavy load, likely for construction purposes.

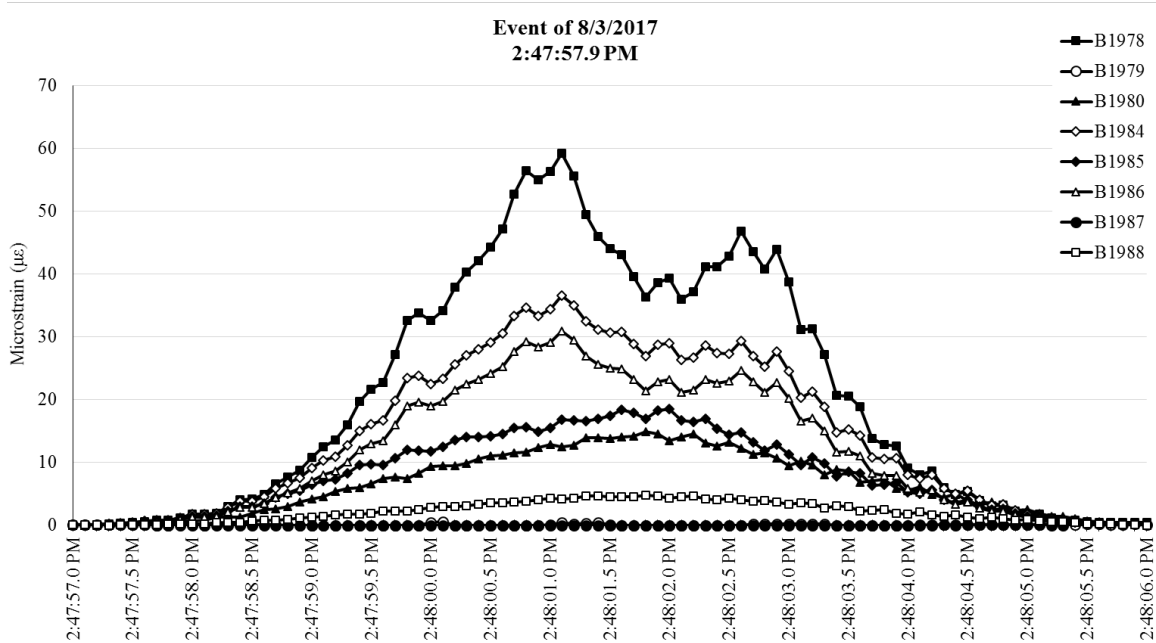


Figure 3.25 Largest recorded strain event

3.4.4 Comparison of Large Strains with Design Loading

In order to compare strain magnitudes with a vehicle of a known weight, a live load test was conducted using an International 7700 dump truck. The axle configuration of the truck is shown in Figure 3.24; an image of the dump truck used is shown in Figure 3.25.

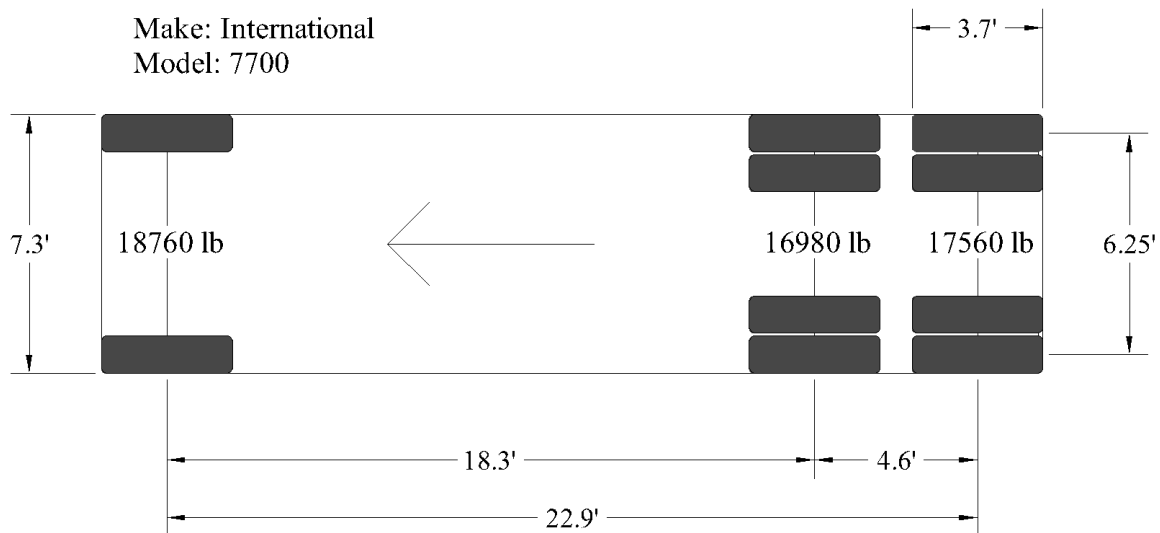


Figure 3.26 Axle configuration of the International 7700 dump truck



Figure 3.27 Image of the International 7700 dump truck used

The dump truck was driven over the bridge along five different load paths. Each load path placed the front-right tire of the dump truck directly over Girders 2, 3, 4, 5, and 6. These load paths were chosen because the test took place on July 18, 2017, and the corresponding girders were the only ones being monitored at the time. (A load path over Girder 1 was not tested, as the truck would have had to drive up onto the sidewalk.) The dump truck drove along each load path twice, and the results were averaged for each load path.

The dump truck caused the largest strain in the bridge when it was positioned with its right tire directly over Girder 5, placing it approximately in the center of the bridge. When positioned there, the truck caused a maximum strain of $33.12 \mu\epsilon$ in Girder 5, but only $13.14 \mu\epsilon$ in Girder 4. When the truck remained in the north lane, it caused a maximum strain of approximately $30.29 \mu\epsilon$ in Girder 4. A more detailed analysis and report on the live load test results will be published at a future date.

While a more detailed analysis of the live load test incorporating a finite element model will be conducted in the future, it can be shown using statics that the dump truck caused a maximum moment of approximately 412.57 kip-feet (559.37 kN-m) in the bridge. Assuming the relationship between the maximum moment caused by a vehicle and the maximum strain induced in the bridge is linear, the strain caused by the dump truck can be used to approximate the strain caused by other types of loading.

For example, an HS-20 truck would create a moment of 604.61 kip-feet (819.74 kN-m) in the bridge. The ratio between the two moments is 1.465, meaning that an HS-20 truck should cause a maximum strain of $42.23 \mu\epsilon$ in Girder 4 ($30.29 \mu\epsilon * 1.465 = 42.23 \mu\epsilon$) if it were driven across the north lane. The controlling HL-93 design loads (consisting of an HS-20 truck plus a lane load of 650 lbs/foot (9340.10 N/m)) would cause an approximate strain of $62.59 \mu\epsilon$ in the bridge.

The calculated moments above assume a partial fixity of 90% at the ends of the bridge girders. However, the fixity of the bridge makes relatively little difference to the moment ratios. For example, the moment ratio between the HS-20 truck and the dump truck is 1.394 if the bridge is completely pinned and 1.486 if the bridge is completely fixed. For the HL-93 design loads and the dump truck, these ratios are 2.067 if pinned and 2.066 if fixed.

Because the moments and strains caused by an HS-20 truck and the controlling HL-93 design loads are an integral part of bridge design, it is significant to note that the traffic at Nibley Bridge regularly exceeded the strains the AASHTO truck loadings should cause. For example, if an HS-20 truck crossed the Nibley Bridge in the north lane, it could be expected to cause a strain of 42.23 $\mu\epsilon$ in Girder 4. During the five weeks of recording, 58 vehicles caused a strain greater than 42.23 $\mu\epsilon$. This accounts for 0.18% of all vehicles that crossed the bridge in the north lane during this period.

The HL-93 design loads would be expected to induce a strain of 62.59 $\mu\epsilon$ in Girder 4. While no events ever exceeded 62.59 $\mu\epsilon$, the maximum recorded strain in Girder 4 was 59.26 $\mu\epsilon$. This comes within 5.61% of exceeding the design loads for the bridge. Considering the relatively short monitoring window of five weeks, it is safe to assume that the design loads could be periodically exceeded every year.

These findings are consistent with the studies on which the bridge design code is based. According to Nowak and Collins, the current bridge code is based off of surveys on highway loadings in 16 different locations. In these surveys, approximately 0.003% of vehicles exceeded HL-93 loading for a 90-foot (27.43-meter) bridge. With 54,896 recorded events over five weeks, the Nibley Bridge could only expect to see a single event exceed the HL-93 loading.

It was expected that the Nibley Bridge did not see any events exceed the HL-93 loading. Because it is in a rural area, the Nibley Bridge sees less traffic than the highway loading surveys. The monitoring window was also smaller for this project than for the surveys used to create the bridge code. Thus, the Nibley Bridge can be expected to see similar results on a smaller scale than the highway surveys.

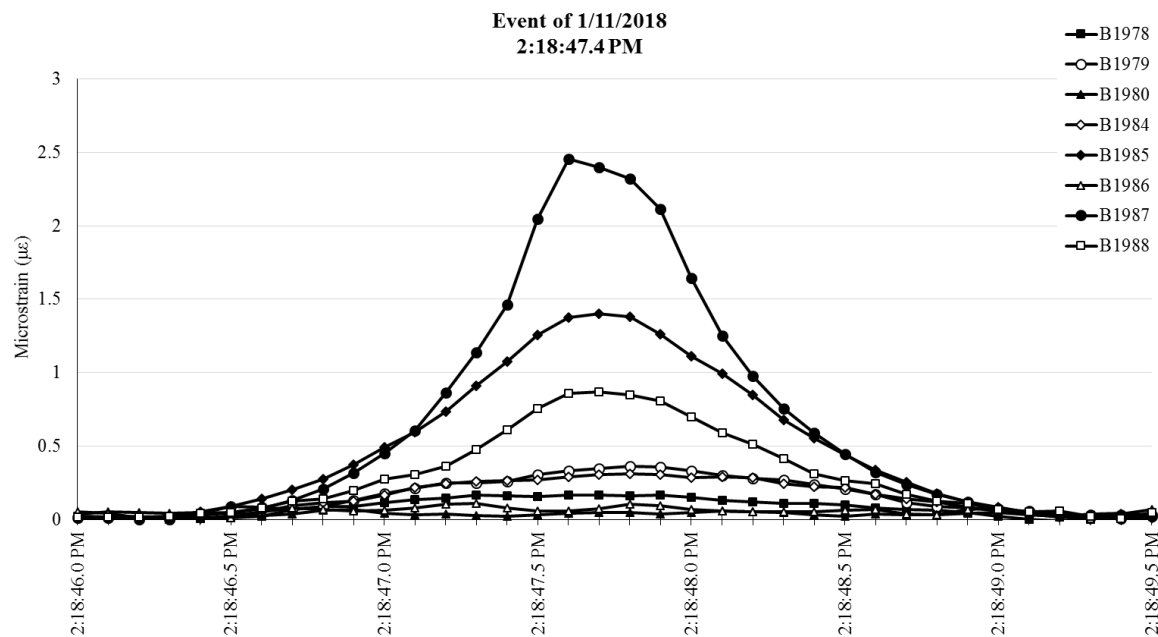
It is also possible the data include larger strains than would be considered normal for the Nibley Bridge. As noted, the Utah Department of Transportation was doing construction on a portion of UT-165 near the Nibley Bridge during the monitoring window. Because of this, an abnormally high number of construction vehicles could be skewing the data.

3.4.5 Vehicle Strain Comparisons

Using the video recorded by the GoPro video monitoring done in Section 3.3.4, strain events were associated with the different vehicle types that caused them. Table 3.3 shows strain data corresponding to each vehicle type. Figures 3.26-3.29 graphically show strain events associated with typical sedans, school buses, semis, and dump trucks. “Typical” events were found by calculating the median for the maximum strain values caused by each vehicle type, then choosing an event whose maximum value was close to the median value.

Table 3.3 Vehicle strain data

Vehicle Type	Mean ($\mu\epsilon$)	Median ($\mu\epsilon$)	Standard Deviation ($\mu\epsilon$)	Minimum ($\mu\epsilon$)	Maximum ($\mu\epsilon$)	# Samples
Sedans	2.417	2.282	0.551	1.099	4.529	100
Minivans	2.874	2.882	0.457	1.893	3.716	17
Jeeps	2.882	2.887	0.401	2.124	3.409	8
SUVs	3.029	3.054	0.540	2.034	4.269	29
Suburbans	3.249	3.237	0.504	2.322	4.654	32
Vans	3.315	3.237	0.404	2.912	3.833	6
Pickup Trucks	3.454	3.372	0.566	2.582	5.051	27
Delivery Trucks	5.733	5.882	0.556	5.000	6.168	4
Semi-Truck	13.350	12.542	2.265	11.599	15.908	3
School Buses	13.729	13.649	1.949	11.212	16.581	11
Dump Trucks	39.218	42.621	7.808	30.286	44.748	3

**Figure 3.28** Strain event from a sedan

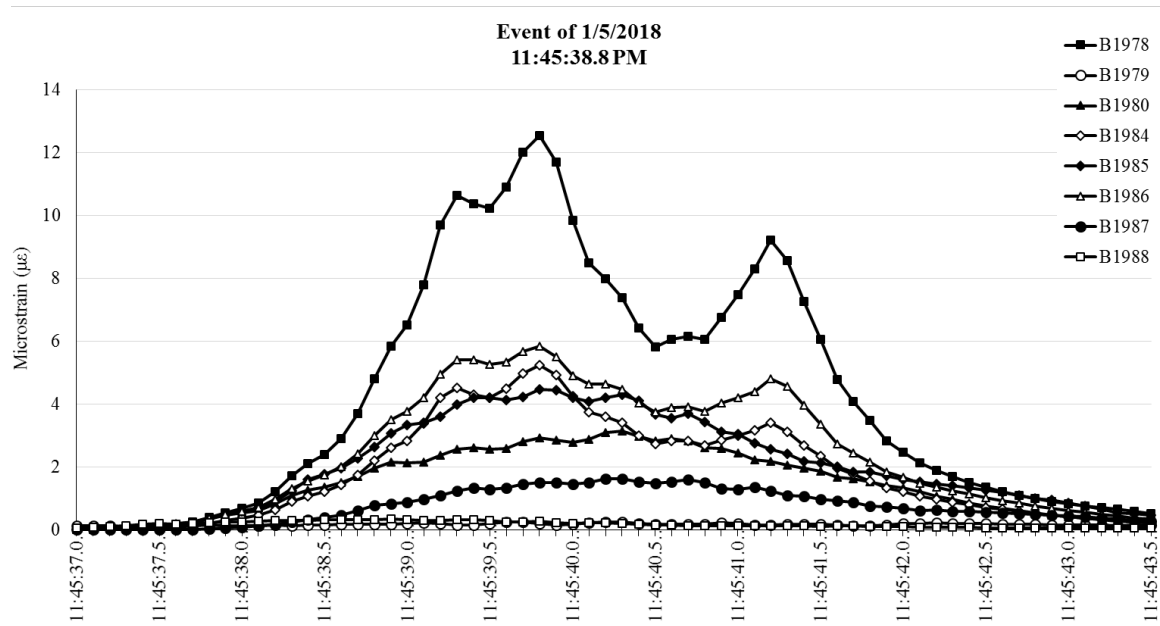


Figure 3.29 Strain event from a semi-truck and trailer

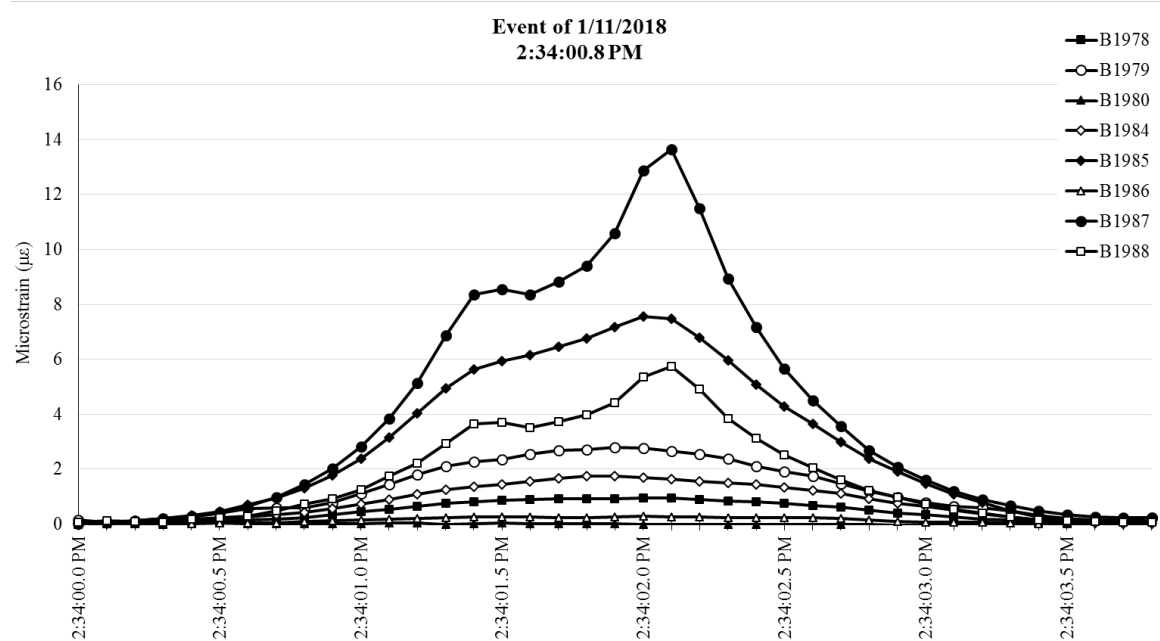


Figure 3.30 Strain event from a school bus

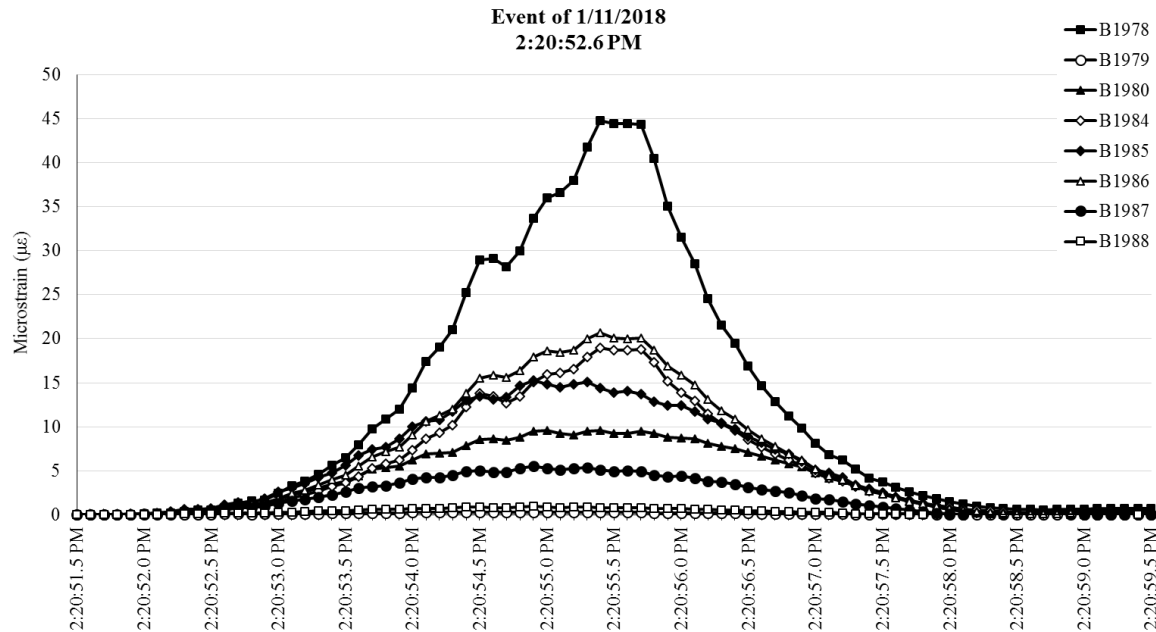


Figure 3.31 Strain event from a dump truck

The data in Table 3.3 show there is little variation in the strains caused by smaller vehicles; sedans, minivans, jeeps, SUVs, suburbans, vans, and pickup trucks all had mean strains that fell between 2.42 and 3.45 $\mu\epsilon$. Most school buses tended to cause a strain of 13.73 $\mu\epsilon$, while semis caused a strain of 13.35 $\mu\epsilon$. Dump trucks caused the highest strain of all, 39.22 $\mu\epsilon$. However, it should be noted that the sample size for both semi-trucks and dump trucks was limited. Given the variability in gross vehicle weight for both vehicle types, it is expected that the strain caused by each vehicle would vary greatly as well.

Figures 3.26, 3.17, 3.28, and 3.29 also demonstrate that as a vehicle's size and weight increases, it becomes possible to distinguish the strains caused by each vehicle axle. This is partially because the increased spacing between the axles prevents the axles from effectively acting as a single force and partially because larger vehicles cross the bridge at a lower speed, allowing for more points to be captured per axle.

3.4.6 Frequency Histograms

The data from all five weeks of recording were combined and analyzed to create frequency histograms of the strains in each girder. Figures 3.30-3.40 show these frequency histograms. The histograms have been divided into bins with a range of 1.0 $\mu\epsilon$ each. Each histogram uses this spacing between 0 and 10 $\mu\epsilon$. After approximately 7 $\mu\epsilon$, the bins level out and most bins afterward account for less than 0.1% of the events.

After 10 $\mu\epsilon$, the graphs contain a bin between 10 and 42.2 $\mu\epsilon$. A strain of 42.2 $\mu\epsilon$ (corresponding with an HS-20 truck) has been included for comparison purposes. The final bin, extending from 42.2 to 59.3 $\mu\epsilon$, recorded the percentage of events whose strains exceed that of an HS-20 truck.

It is important to note that each histogram shows the strain in the girder for every event where any sensor crossed the 1.0 $\mu\epsilon$ threshold. This is why the bins from 0-1 $\mu\epsilon$ contain the highest percent of events for every girder. If a light vehicle crosses the Nibley Bridge in the south lane, it will not cause noticeable strain in the girders on the north end of the bridge. However, it will still contribute to the histograms for the north girders. Thus, the high percentages in the 0-1 $\mu\epsilon$ range are not due to exceptionally light vehicles; rather, they are related to the positioning of the vehicles on the bridge.

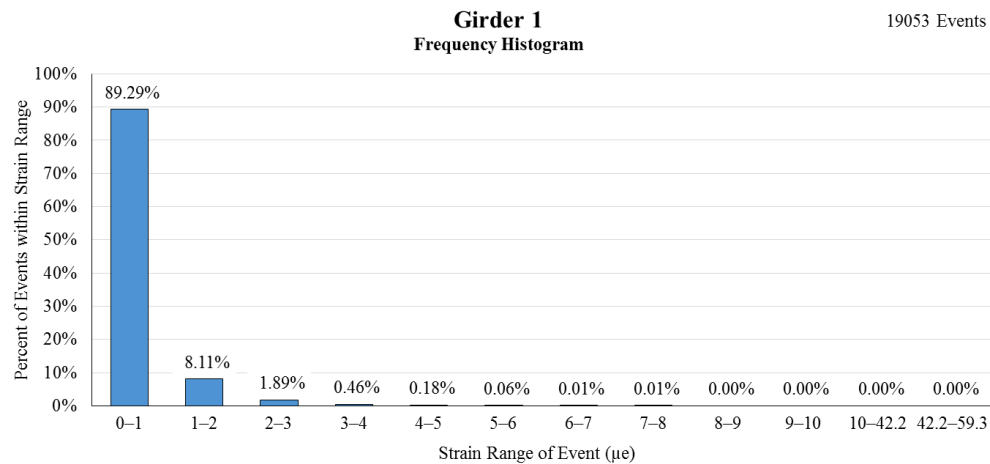


Figure 3.32 Frequency histogram of recorded strains in Girder 1

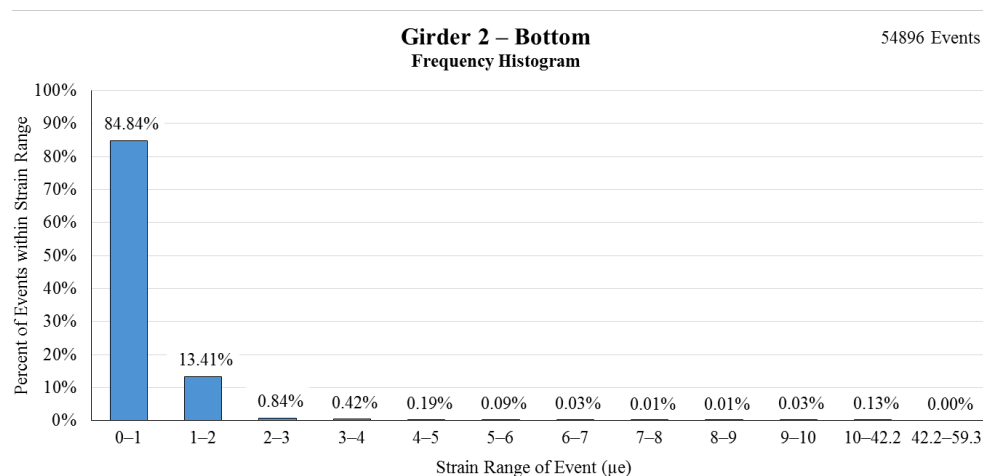


Figure 3.33 Frequency histogram of recorded strains at the bottom of Girder 2

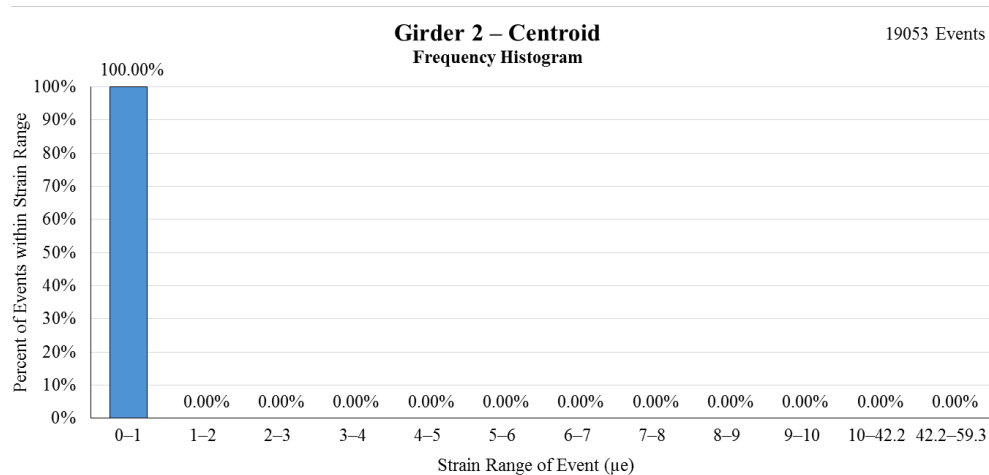


Figure 3.34 Frequency histogram of recorded strains at the centroid of Girder 2

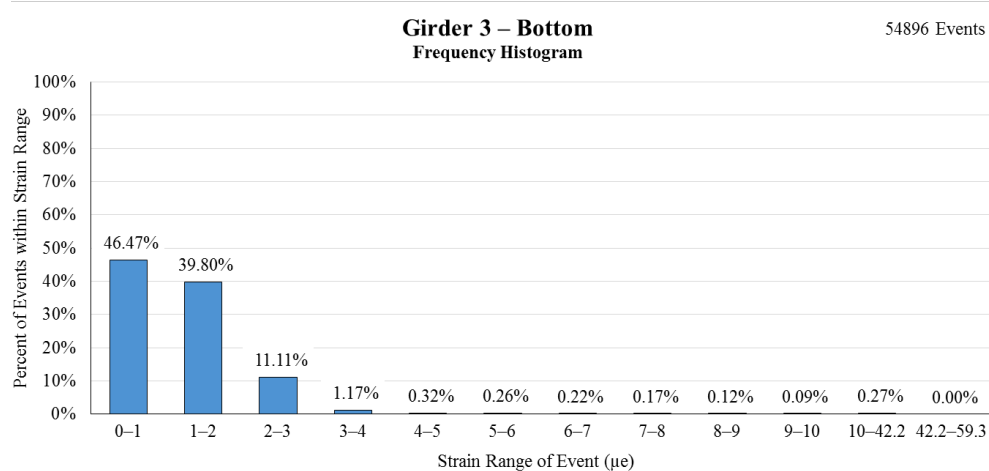


Figure 3.35 Frequency histogram of recorded strains at the bottom of Girder 3

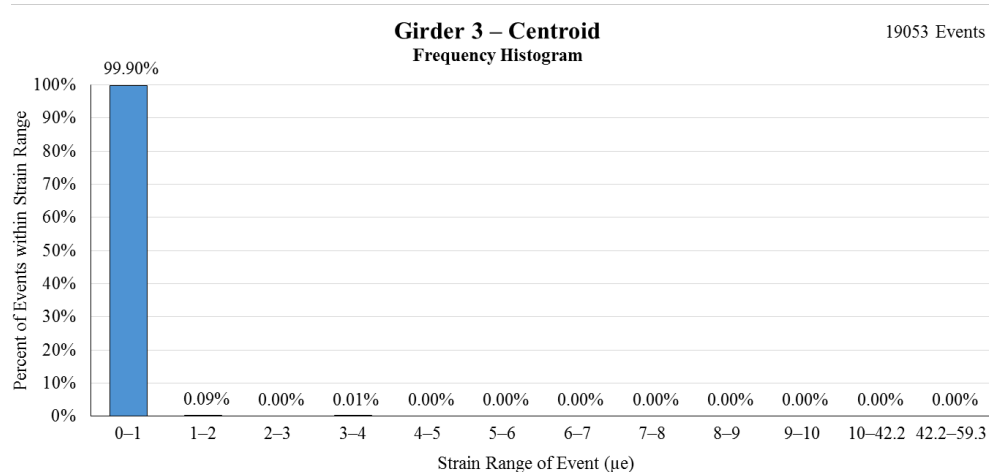


Figure 3.36 Frequency histogram of recorded strains at the centroid of Girder 3

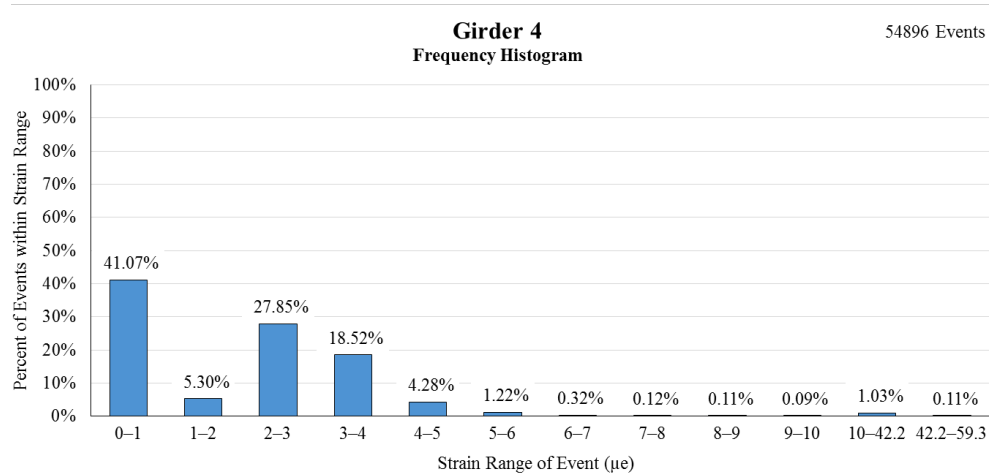


Figure 3.37 Frequency histogram of recorded strains in Girder 4

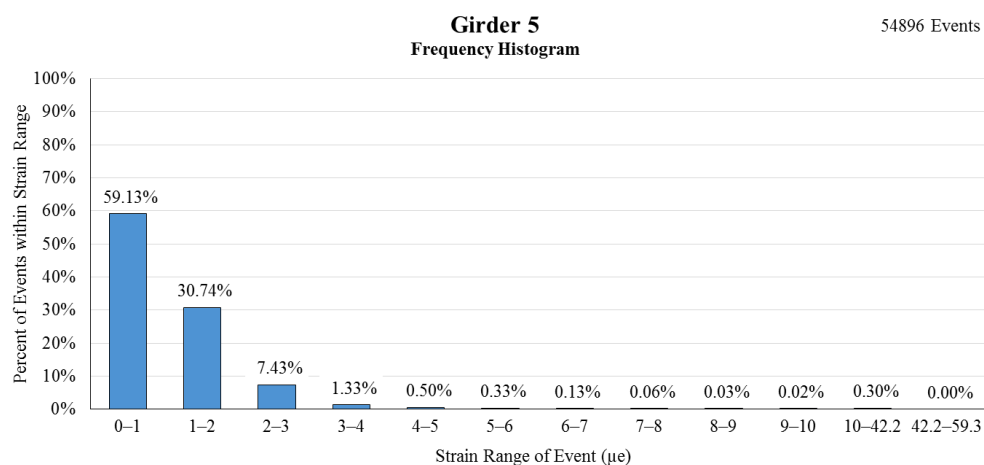


Figure 3.38 Frequency histogram of recorded strains in Girder 5

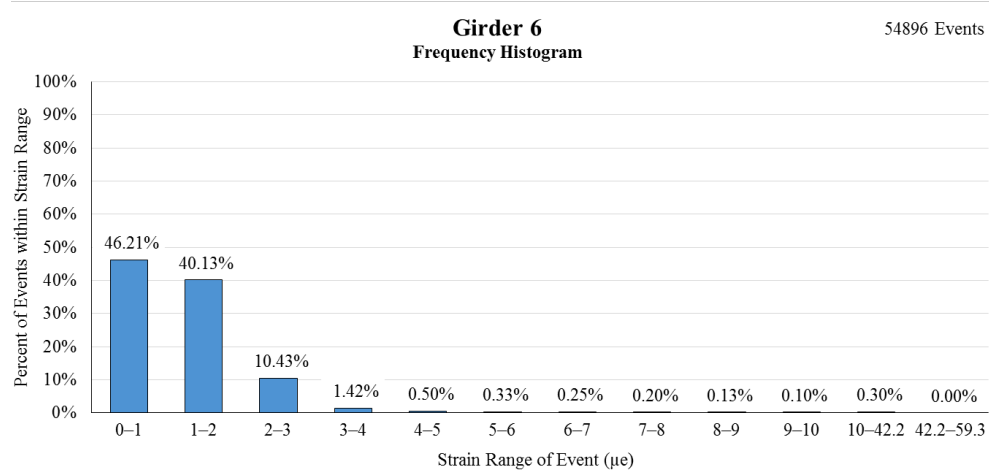


Figure 3.39 Frequency histogram of recorded strains in Girder 6

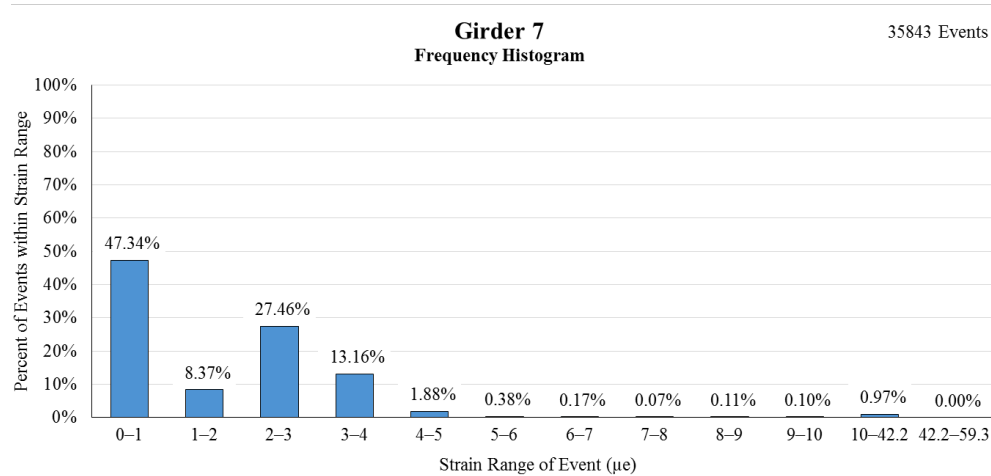


Figure 3.40 Frequency histogram of recorded strains in Girder 7

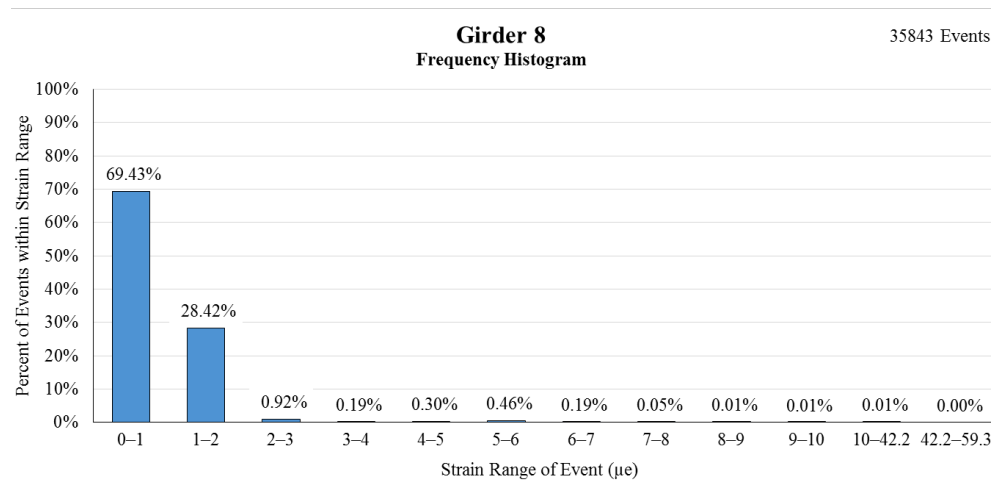


Figure 3.41 Frequency histogram of recorded strains in Girder 8

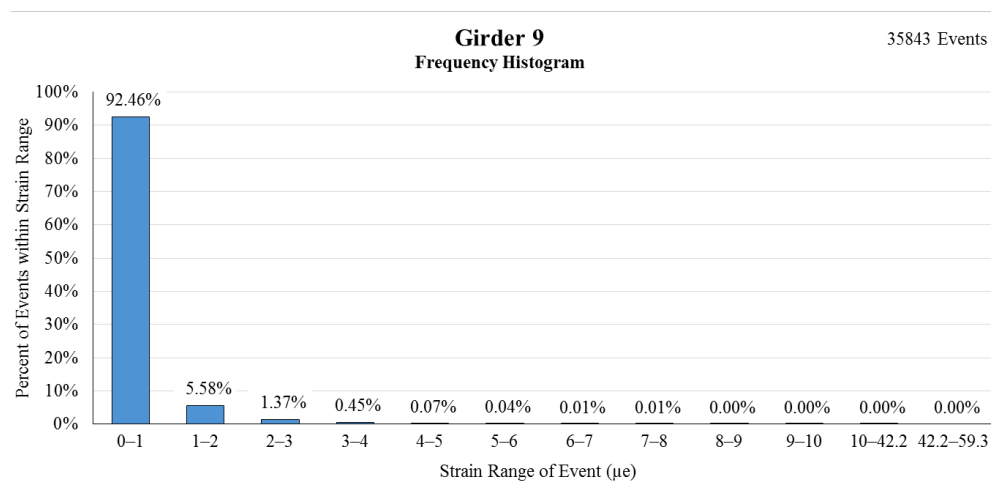


Figure 3.42 Frequency histogram of recorded strains in Girder 9

As expected, the sensors located at the centroids of Girders 2 and 3 recorded zero strain 99.9% of the time. This is because there is no strain due to moment at the elastic neutral axis of a girder. The events where the strains are greater than $1.0 \mu\epsilon$ are likely due to either excessive noise in the sensors or errors in the data processing programs.

The monitored exterior girder, Girder 1, also experienced little to no strains. This is because Girder 1 lies directly beneath the sidewalk, where there are few heavy loads. Girder 1's largest recorded strain, $7.24 \mu\epsilon$, was the result of an even larger strain in Girder 4, $52.78 \mu\epsilon$. In fact, the three outside girders along each side of the bridge all experienced their strains as a result of higher loading in a nearby girder. Analysis shows that 97.70% of strains in Girders 1, 2, 3, 8, and 9 above $5.0 \mu\epsilon$ were caused by larger strains in other girders.

The histograms show that the level of strain a girder experiences is a direct function of where the girders are positioned in relation to the traffic lanes. The girders directly beneath the traffic lanes experienced much higher levels of strain than girders positioned farther away. The histograms also reflect the symmetry of the bridge. Girders 4 and 7 have similar histograms, as do Girders 5 and 6, Girders 2 and 9, etc.

After analysis of Figures 3.30-3.40 was complete, a frequency histogram (Figure 3.41) and normalized distribution plot on probability paper (Figure 3.42) were created using the maximum strain in any girder on the bridge for each event. Unlike Figures 3.30-3.40 above, Figures 3.41 and 3.42 do not consider the positioning of the vehicle on the bridge. Instead, the data are directly related to the gross vehicle weight (GVW) of the vehicles crossing the Nibley Bridge. Because the event extraction program ignored strains below $1.0 \mu\epsilon$, none of the maximum strains were below $1.0 \mu\epsilon$.

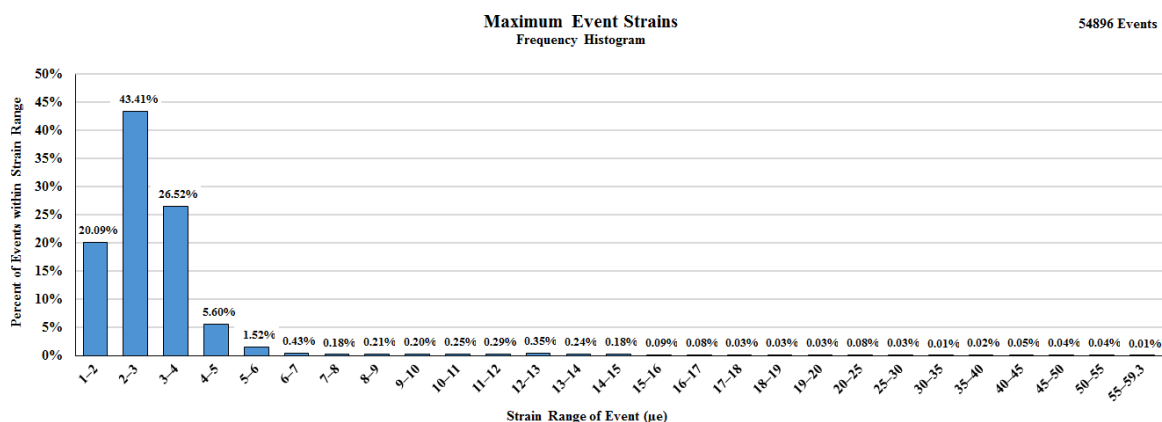


Figure 3.43 Frequency histogram of maximum recorded event strains in any girder

Figure 3.41 shows that the vast majority of vehicles (95.62%) cause less than $5.0 \mu\epsilon$ strain in the bridge. The frequency of strain events flattens out after approximately $7 \mu\epsilon$. However, there are clusters of vehicles at approximately $12.5 \mu\epsilon$, $22.5 \mu\epsilon$, $42.5 \mu\epsilon$, and $52.5 \mu\epsilon$. The cluster of vehicles at $12.5 \mu\epsilon$ most likely corresponds to school buses and semis crossing the bridge. Likewise, the clusters of vehicle strains at $22.5 \mu\epsilon$, $42.5 \mu\epsilon$, and $52.5 \mu\epsilon$ likely correspond to construction equipment.

Figure 3.42 plots the distribution of the maximum strains in the bridge on normal probability paper. From this figure, it can be shown that the vehicles on the bridge caused a mean strain of $2.67 \mu\epsilon$ with a standard deviation of approximately $0.886 \mu\epsilon$. It also reveals a large variation in the intensity of strains that occur on the Nibley Bridge.

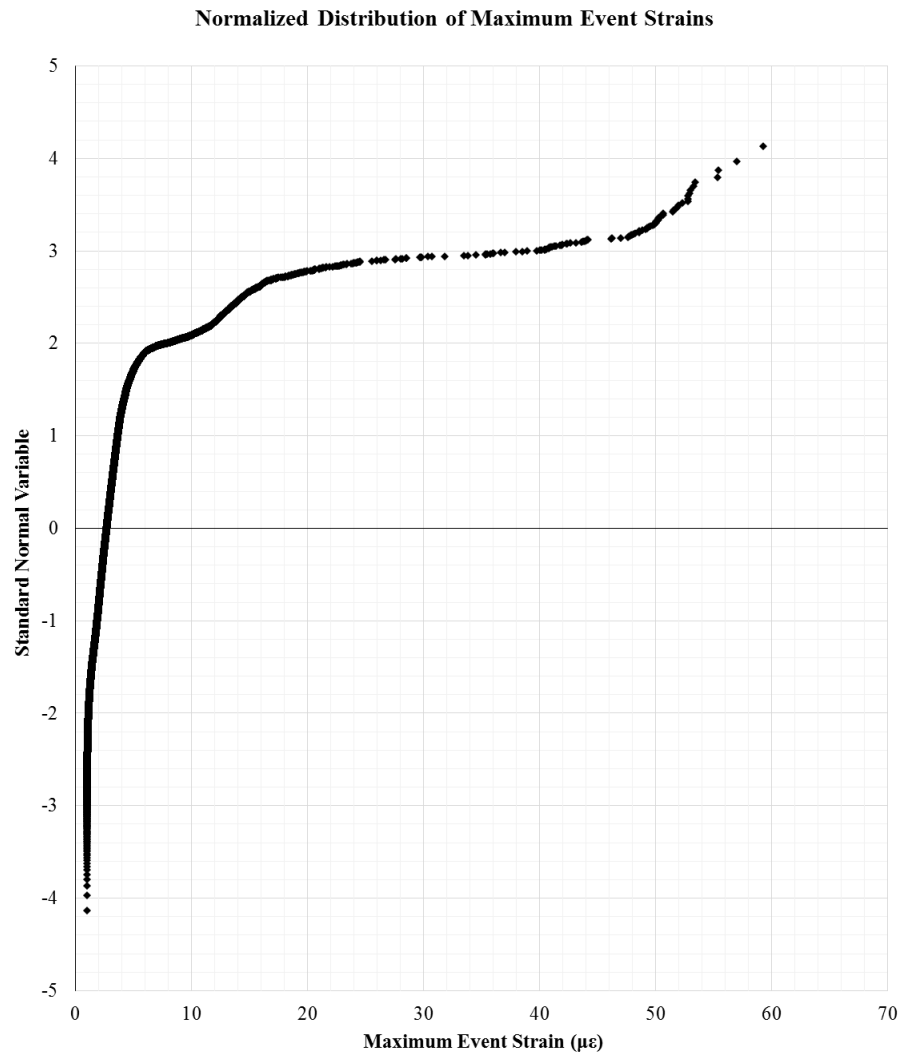


Figure 3.44 Maximum bridge strains plotted on normal probability paper

Comparing Figure 3.42 against Figure 3.43 reveals that the Nibley Bridge traffic data collected closely resemble the lower leg of similar traffic studies done by the Federal Highway Administration (FHWA). This is to be expected, as many of the largest strains that occur on highway bridges are not present in rural Nibley. It also serves to validate the findings of this project by showing that the collected data compare well with previously collected data. (While the horizontal axis of Figures 3.42 and 3.43 are different, the maximum event strain and gross vehicle weight are directly correlated, allowing for a direct comparison.)

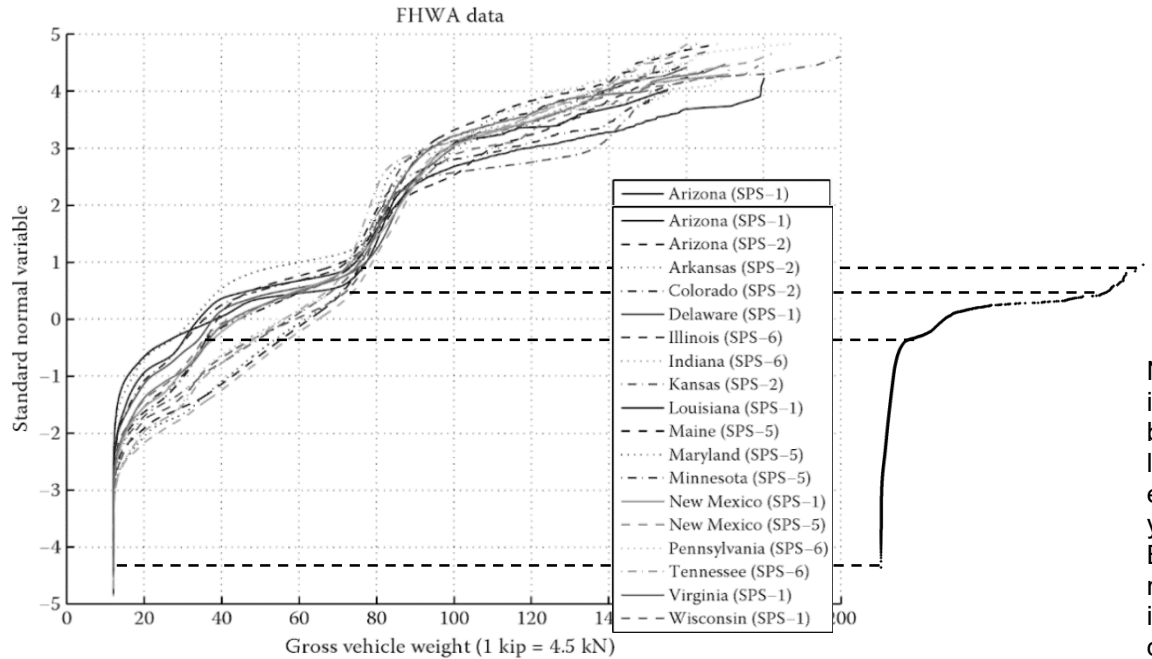


Figure 3.45 GVW of trucks surveyed on roads from 16 different states, annotated (Nowak and Collins, 2013)

3.4.7 Girder Distribution Factors

Using the 54,896 data points collected during the summer and winter, girder distribution factors (GDFs) were calculated for the north and south lanes. This was done by first sorting the events by the lane in which they occurred. Average strain values were then calculated for each girder. The symmetry of the bridge was used to fill in gaps in the data. Finally, the girder distribution factors were calculated using Equation 2. The multiple presence factor, m , equals 1.2 when a single lane is loaded and 1.0 when both lanes are loaded. The results are shown graphically in Figures 3.44 and 3.45.

$$GDF_i = m \frac{\varepsilon_i}{\sum \varepsilon_i}$$

Equation 2

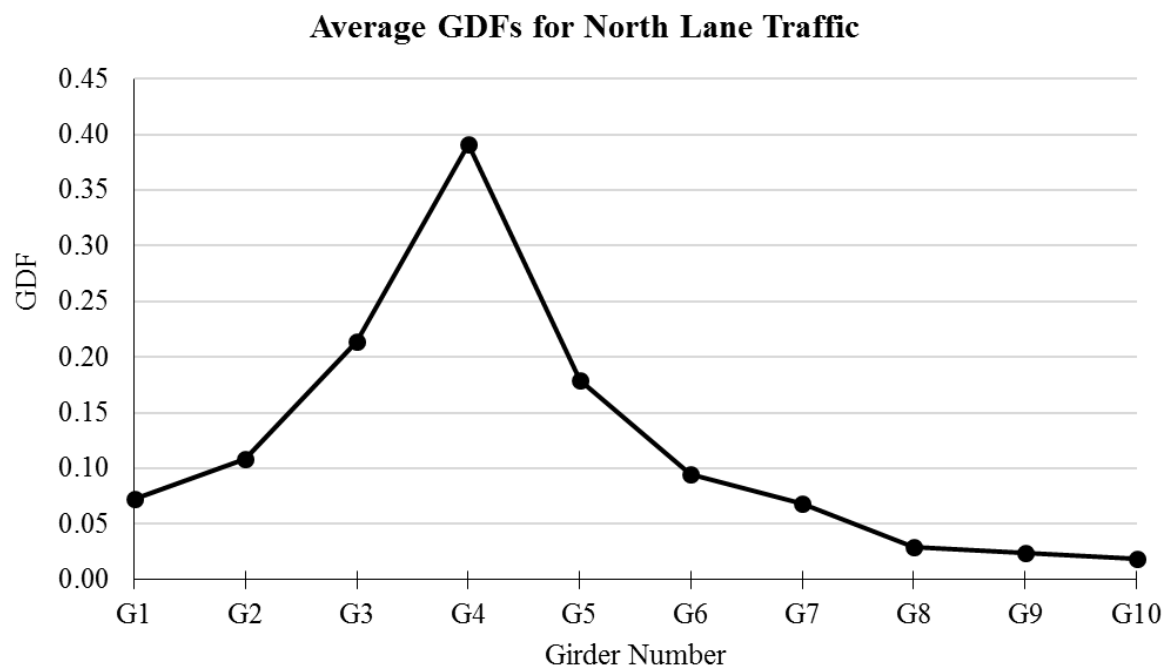


Figure 3.46 Girder distribution factors for north lane

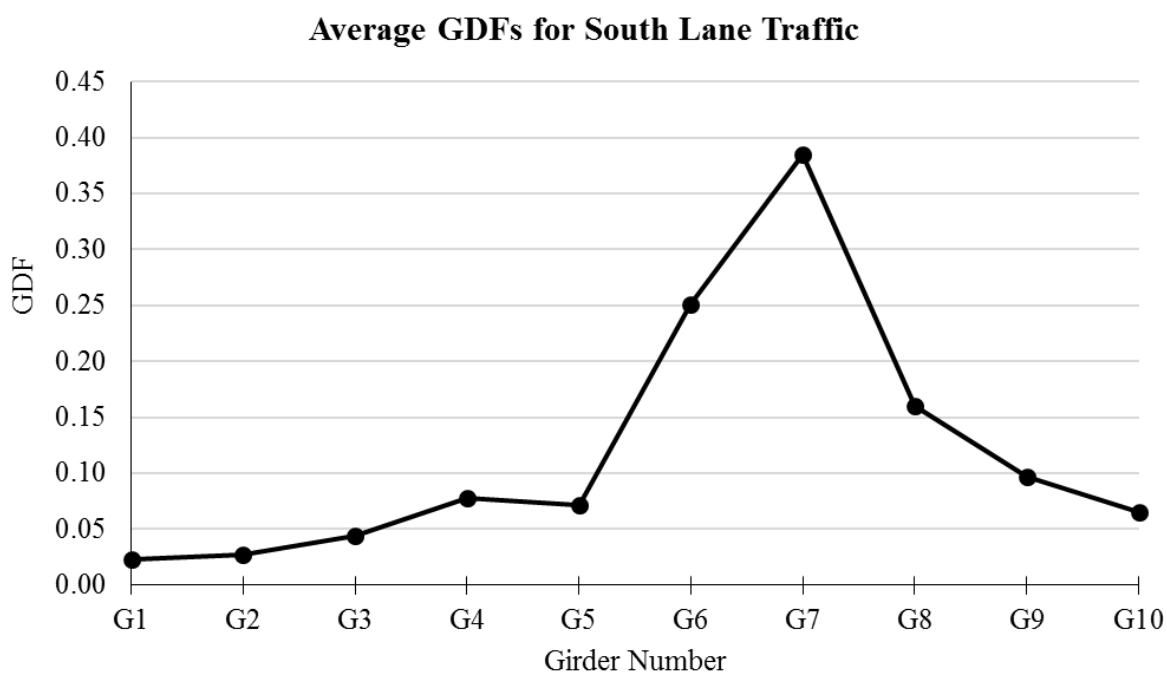


Figure 3.47 Girder distribution factors for south lane

Figures 3.44 and 3.45 show that the girders directly below the traffic lanes typically carried the majority of the load. The fourth girders in from each end typically carried approximately 32.3% of the load by themselves. All other girders carried less than 25% of the load, and the girders on the farthest side of the bridge from the loaded lane typically did little to carry the load.

The calculated girder distribution factors for the south lane appear to be slightly skewed to favor the girders on the north end of the bridge. In Figure 3.45, Girder G6 takes a higher share of the load than its symmetric girder, Girder 5, does in Figure 3.44. The girder distribution factor for Girder 4 in the south lane is higher than that of Girder 5, which seems incorrect. This could support the theory that Sensor B1978 attached to Girder 4 has malfunctioned and needs to be calibrated.

By adding the average strains from each lane together, girder distribution factors for multiple loaded lanes can be calculated. The girder distribution factor for loading multiple lanes is shown in Figure 3.46. As can be seen, loading multiple lanes does not significantly impact the girder distribution factors for the worst-case girders, Girders 4 and 7. Table 3.4 numerically contains the data shown in Figures 3.44, 3.45, and 3.46.

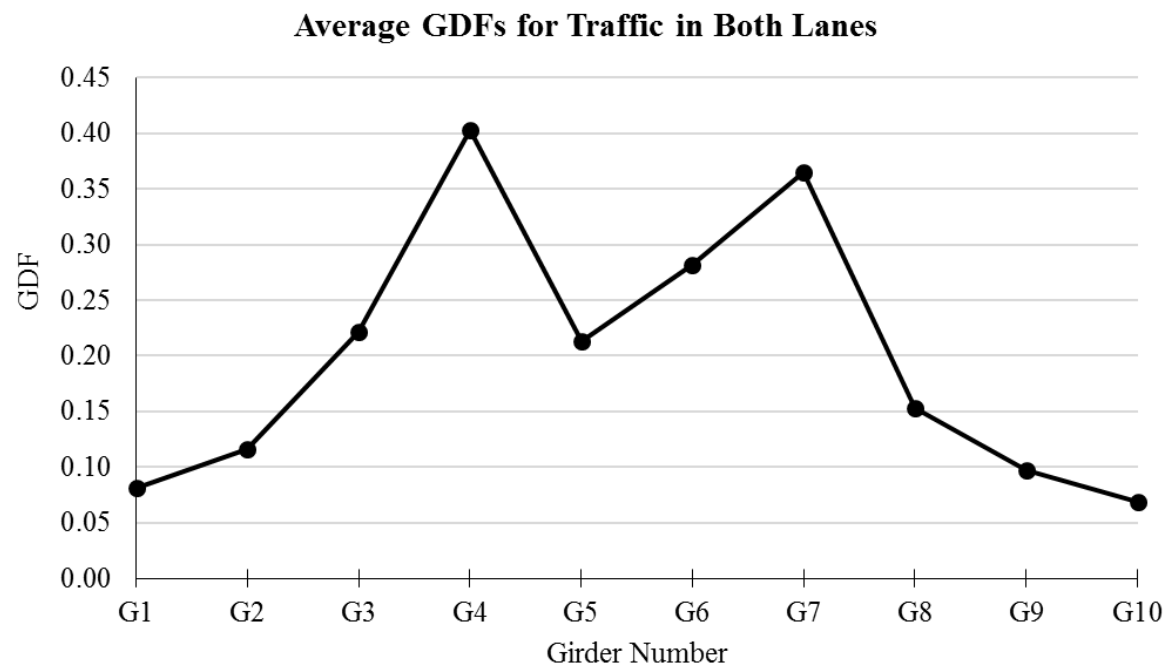


Figure 3.48 Girder distribution factors for multiple loaded lanes

Table 3.4 Girder distribution factors

Girder	G1	G2	G3	G4	G5	G6	G7	G8	G9	G10
North Lane	0.0728	0.1082	0.2134	0.3916	0.1793	0.0945	0.0681	0.0292	0.0235	0.0193
South Lane	0.0225	0.0275	0.0442	0.0774	0.0711	0.2509	0.3849	0.1603	0.0963	0.0648
Multiple Lanes	0.0814	0.1163	0.2215	0.4034	0.2130	0.2817	0.3648	0.1527	0.0970	0.0682

Comparing the controlling girder distribution factors from Table 3.4 against the AASHTO LRFD Bridge Design Specifications (4th Edition) reveals that the girder distribution factors for a single lane are appropriately conservative. For a bridge with the Nibley Bridge's specifications, the code requires a GDF of 0.4014 for a single loaded lane; the controlling single-lane GDF was 0.3916.

However, the AASHTO design GDF for when multiple lanes are loaded is 0.5506. The controlling measured GDF for this scenario was only 0.4034. Thus, the girder distribution factor for multiple loaded lanes is overly conservative by 36.51%.

3.5 Long-Term Prestress Losses

Strain data were taken at three elevation locations on an interior girder (Site D) and an exterior girder (Site B). The change in strains was recorded for approximately 80 days. At each instrumentation cross section, two strain gauges were placed in the girder web (shown in Figure 3.10 as UW and LW) and the remaining two at the bottom of the girder. At Sites B and D, gauges BR and BL corresponded to the centroid of the prestressing steel. UW is located 61 cm (24 in.) from the bottom of the girder and LW is located 44 cm (17-3/8 in.) from the bottom. BL and BR are located 10 cm (3-3/4 in.) from the bottom and 18 cm (7 in.) from the centerline.

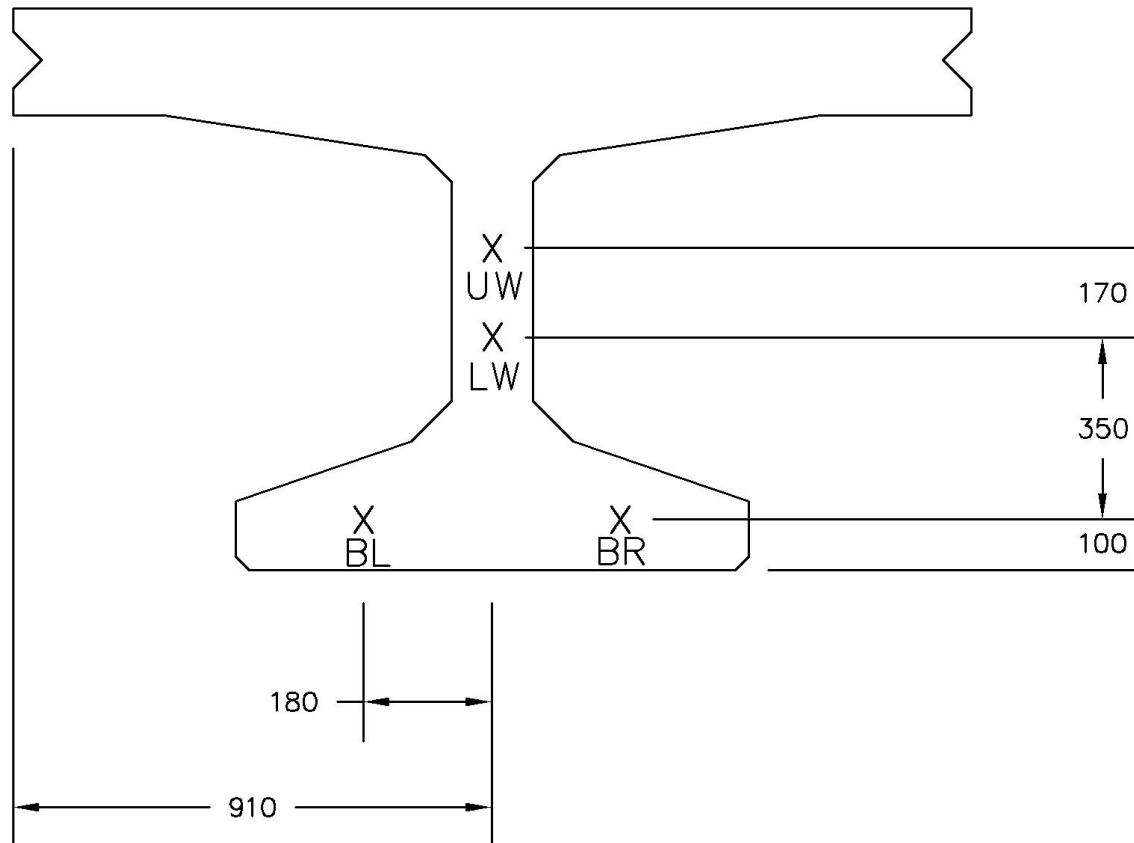


Figure 3.49 Typical girder instrumentation plan (dimensions in mm)

Figure 3.47 and Figure 3.48 show the changes in strain measured at mid-span for Girders 1 and 5 for the duration of this study. These plots show the change in strain was higher in the lower gages in comparison with those in the webs. This is due to the higher prestressing at the bottom of the girders. The changes in strain at the centroid of the prestressing strands for the two girders were used to determine the change in prestress. Girder D experienced a larger increase in strain over time in comparison with Girder B (Figure 3.50).

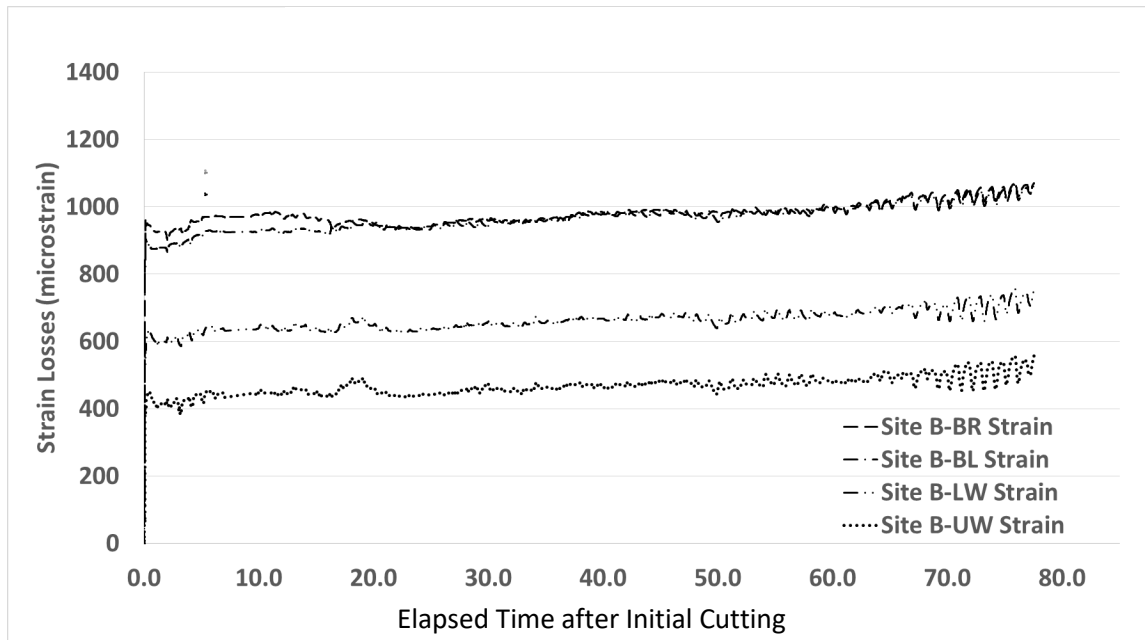


Figure 3.50 Long-term prestressing steel strain losses at mid-span for Girder 1

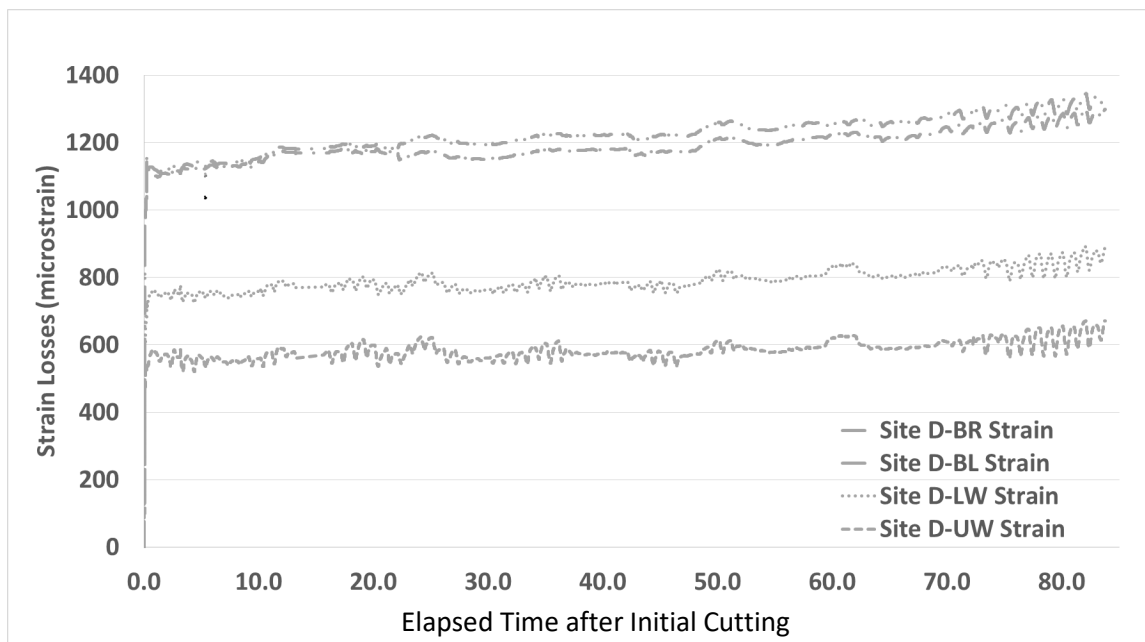


Figure 3.51 Long-term prestressing steel strain losses at mid-span for Girder 5

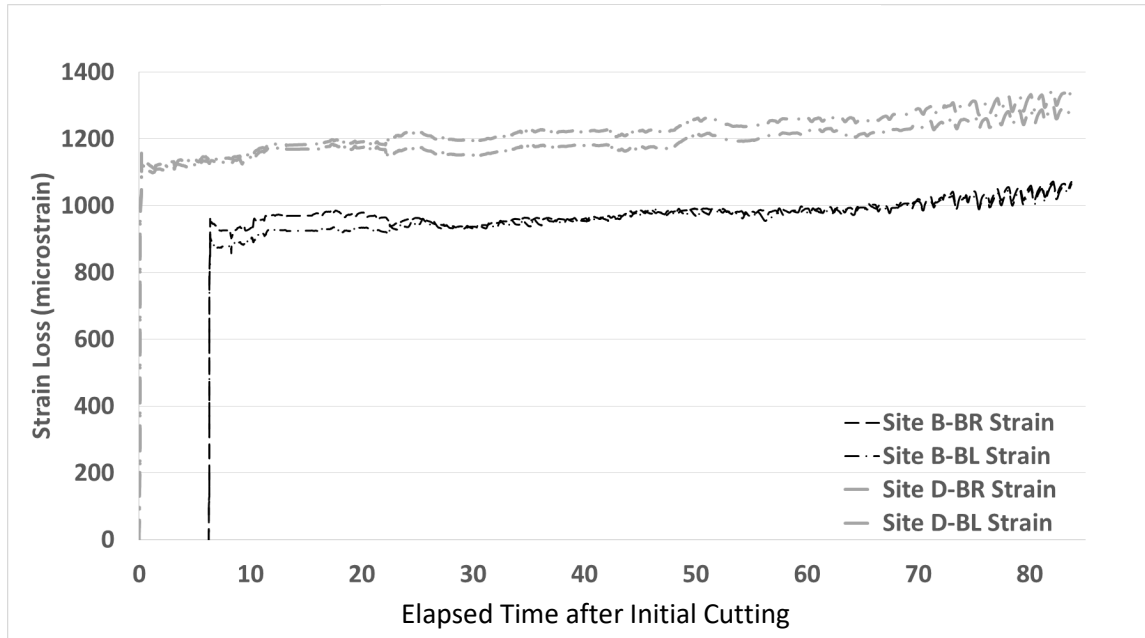


Figure 3.52 Long-term prestressing steel strain losses at mid-span for Girders 1 and 5

As shown in Fig. 3.47 through Fig. 3.49, the long-term strain losses measured in this study linearly increased after the initial losses occurred. Girder 1 experienced an overall average 220.3 microstrain larger strain loss than Girder 5. The maximum and minimum differences were 262.4 microstrain and 128 microstrain, respectively. This difference occurred with the short-term losses, as the long-term rate of loss for both girders is approximately the same.

Predicted losses using the AASHTO LRFD Refined Method and AASHTO LRFD Approximate Method were compared against the measured losses and are shown in Figure 3.51.

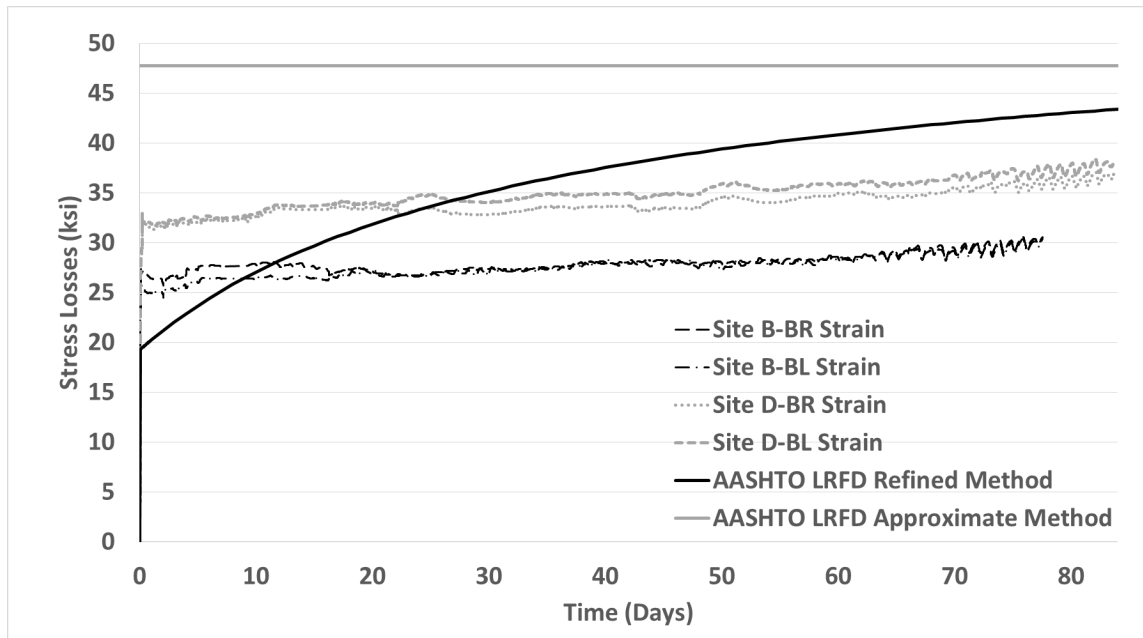


Figure 3.53 Mid-span stress loss comparisons

Figure 3.51 shows that the AASHTO LRFD Approximate Method over-predicted the long-term losses. This method provides a lump-sum value of losses at the service limit state to be taken as the effective prestress force for design. In comparison, the AASHTO LRFD Refined Method under-predicted the short-term losses (elastic shortening losses) and tended to over-predict the long-term losses. The underprediction of the short-term losses can be attributed to an over-estimation of the elastic modulus of the concrete. The over prediction of the long-term losses can be attributed to over-prediction of the creep and shrinkage losses. Overall, the long-term prestress losses for Site B and Site D were over-predicted by 31.5% and 11.1%, respectively.

4. CONCLUSION

4.1 Summary of Conclusions

4.1.1 Summary of Conclusions for Short- and Long-Term Strain Monitoring Research

Based on the measured data, traffic on the Nibley Bridge regularly exceeded HS-20 truck loading, with recorded strains of up to $59.26 \mu\epsilon$. The largest loading events approached (but did not exceed) the HL-93 design loads. Because the monitoring took place over a relatively narrow span of time, it was theorized the maximum strains experienced by the bridge girders could be even higher than the measured values.

It was discovered that the largest strains were typically concentrated into a small number of days per week. On any given day, the largest strains were of similar magnitudes, and the shape of the strain events indicated the strains were caused by vehicles with similar axle configurations (See Figure 3.22). Because of these similarities, it was theorized that the largest strain events on any given day were likely caused by the same vehicle crossing the Nibley Bridge multiple times that day.

It was found that the girders immediately under the traffic lanes experienced the highest magnitude of strains. Adjacent girders experienced progressively less strain the farther they were placed from the loaded traffic lane. The girders farthest from the loaded traffic lane (the exterior girders and girders underneath in the opposite lane) typically experienced little to no strain.

As expected, the distribution of strain events followed established traffic patterns, with the number of strain events picking up throughout the day and decreasing at night. The highest number of strain events occurred just before school started and right after school let out. During these periods, multiple vehicles used the bridge at once, resulting in higher strains in the bridge girders.

The majority of vehicles (95.62%) caused less than $5.0 \mu\epsilon$ of strain in any girder on the bridge. These values reflect smaller vehicles crossing the Nibley Bridge; vehicles smaller than a pickup truck typically caused a strain of $2.42\text{--}3.45 \mu\epsilon$. School buses typically caused a strain of around $13.65 \mu\epsilon$, while heavily laden construction equipment caused the largest strains, but had highly variable strain magnitudes.

Long-term changes in strain were monitored and used to calculate the long-term changes in prestress for an exterior and interior girder. In general, the elastic shortening losses were under-predicted. This was likely due to an overestimation of the elastic modulus of the concrete. For both the interior and exterior girders, the long-term prestress losses were over-predicted by the AASHTO LRFD methods. The over-prediction of the long-term losses can be attributed to over-prediction of the creep and shrinkage losses. Overall, the long-term prestress losses for Site B and Site D were over-predicted by 31.5% and 11.1%, respectively, for the AASHTO LRFD Refined Method.

REFERENCES

- agisoft. (2014). “Ortli excavation site (low-poly).” Sketchfab, New York, NY.
- Dà-Jiāng Innovations. (2017). Phantom 4 Pro. *www.dji.com, photograph*, Dà-Jiāng Innovations Science and Technology Co., Ltd, Shenzhen, China.
- Dà-Jiāng Innovations. (2017). Remote Controller with Built-in Screen. *www.dji.com, photograph*, Dà-Jiāng Innovations Science and Technology Co., Ltd, Shenzhen, China.
- Dà-Jiāng Innovations. (2018). “DJI Phantom 4 Pro – Specs, FAQ, Tutorials and Downloads.” DJI Official Website, Dà-Jiāng Innovations, <<https://www.dji.com/phantom-4-pro/info#specs>> (Mar. 28, 2018).
- DroneDeploy Labs. (2017). “DroneDeploy.” *DroneDeploy*, computer software, Infatics, Inc.
- Hodson, D. J., Barr, P. J., and Halling, M. W. (2012). “Live-Load Analysis of Posttensioned Box-Girder Bridges.” *Journal of Bridge Engineering*, 17(4), 644–651.
- Lattanzi, D., and Miller, G. R. (2015). “3D Scene Reconstruction for Robotic Bridge Inspection.” *Journal of Infrastructure Systems*, 21(2), 04014041–1-04014041–12.
- Ma, Z. (J.), Chaudhury, S., Millam, J. L., and Hulsey, J. L. (2007). “Field Test and 3D FE Modeling of Decked Bulb-Tee Bridges.” *Journal of Bridge Engineering*, 12(3), 306–314.
- Nowak, A. S., and Collins, K. R. (2013). Reliability of Structures. CRC Press, Boca Raton, FL.
- Owens, P. (n.d.). *Perrine Bridge*. <https://visitidaho.org/>, photograph, Idaho Department of Commerce - Tourism, Boise, ID.
- Parrot S.A. (2017). Parrot AR Drone GPS Edition. photograph.
- Pickett, E. (2017). “The Short and Long-Term Effects of Temperature and Strain on a Concrete Bulb-Tee Girder Bridge.” thesis.
- Schwarz, M., and Laman, J. A. (2001). “Response of Prestressed Concrete I-Girder Bridges to Live Load.” *Journal of Bridge Engineering*, 6(1), 1–8.
- Zink, J., and Lovelace, B. (2015). *Unmanned Aerial Vehicle Bridge Inspection Demonstration Project*. Minnesota Department of Transportation, Research Services & Library, St. Paul, MN.

APPENDIX A

Event Extraction VBA Program

```
Sub ExtractEvents()  
    Dim Threshold As Double  
    Dim MaxStallTime As Double  
    Dim NormalDataPath As String  
    Dim EventDataPath As String  
    Dim TestSpecificationName As String  
    Dim PointsPerSecond As String  
    Dim FileLength As Double  
  
    Dim mybook As Workbook, BaseWks As Worksheet, CalcMode As Long  
    Dim MyFiles() As String, FilesInPath As String  
  
    Dim TimeFormula As String  
    Dim NumberEvents As Double  
    Dim FNum As Double  
    Dim StartCell As Double  
    Dim StopCell As Double  
    Dim StartTime As Double  
    Dim FirstEvent As Double  
    Dim EventRow As Double  
    Dim Filename As String  
    Dim BeforeEventTime As Double  
    Dim AfterEventTime As Double  
    Dim CompareTime As Double  
    Dim IgnoreTime As Double  
  
    '*****  
    '*****  
  
    Threshold = Worksheets("Main").Range("D16").Cells(1, 1).Value  
    MaxStallTime = Worksheets("Main").Range("D17").Cells(1, 1).Value  
    BeforeEventTime = Worksheets("Main").Range("D18").Cells(1, 1).Value  
    AfterEventTime = Worksheets("Main").Range("D19").Cells(1, 1).Value  
    CompareTime = Worksheets("Main").Range("D20").Cells(1, 1).Value  
    IgnoreTime = Worksheets("Main").Range("D21").Cells(1, 1).Value  
    NormalDataPath = Worksheets("Main").Range("D24").Cells(1, 1).Value  
    EventDataPath = Worksheets("Main").Range("D25").Cells(1, 1).Value  
    TestSpecificationName = Worksheets("Main").Range("D31").Cells(1,  
        1).Value  
    PointsPerSecond = Worksheets("Main").Range("D32").Cells(1, 1).Value  
    FileLength = Worksheets("Main").Range("D33").Cells(1, 1).Value  
    TimeofYear = Worksheets("Main").Range("D35").Cells(1, 1).Value  
  
    '*****  
    '*****  
  
    FileLength = PointsPerSecond * 3600 * FileLength + 1  
    MaxStallTime = MaxStallTime * PointsPerSecond  
    BeforeEventTime = BeforeEventTime * PointsPerSecond  
    AfterEventTime = AfterEventTime * PointsPerSecond  
    CompareTime = CompareTime * PointsPerSecond  
    IgnoreTime = IgnoreTime * PointsPerSecond
```



```

' Add a slash after path names if needed.
If Right(NormalDataPath, 1) <> "\" Then
    NormalDataPath = NormalDataPath & "\"
End If
If Right(EventDataPath, 1) <> "\" Then
    EventDataPath = EventDataPath & "\"
End If

' If there are no TDMS files in the folder, stop program.
FilesInPath = Dir(NormalDataPath & "*.tdms*")
If FilesInPath = "" Then
    MsgBox "No TDMS files found"
    Exit Sub
End If

' Fill the myFiles array with the list of TDMS files in the folder.
FNum = 0
Do While FilesInPath <> ""
    FNum = FNum + 1
    ReDim Preserve MyFiles(1 To FNum)
    MyFiles(FNum) = FilesInPath
    FilesInPath = Dir()
Loop

' Change application properties.
With Application
    CalcMode = .Calculation
    .Calculation = xlCalculationManual
    .ScreenUpdating = False
    .EnableEvents = False
    .CalculateBeforeSave = False
End With

' Loop through all files in the myFiles array.
If FNum > 0 Then
    For FNum = LBound(MyFiles) To UBound(MyFiles)
        Set mybook = Nothing
        On Error Resume Next
        On Error GoTo 0

        '*****Open TDMS File
        Code*****
        'Get TDM Excel Add-In
        Dim obj As COMAddIn
        Set obj = Application.COMAddIns.Item("ExcelTDM.TDMAddin")

        'Confirm only importing "Description" properties for Root
        Call obj.Object.Config.RootProperties.DeselectAll
        Call obj.Object.Config.RootProperties.Select("Description")

        'Show the group count as property
        Call obj.Object.Config.RootProperties.Select("Groups")

        'Select all the available properties for Group
        Call obj.Object.Config.GroupProperties.SelectAll

        'Import custom properties

```



```

obj.Object.Config.RootProperties.SelectCustomProperties =
    True
obj.Object.Config.GroupProperties.SelectCustomProperties =
    True
obj.Object.Config.ChannelProperties.SelectCustomProperties
    = True

'Import the selected file
Call obj.Object.ImportFile(NormalDataPath & MyFiles(FNum))

'Record down the current workbook & Select Correct Sheet
Set mybook = ActiveWorkbook
'Range("D3") = (Left(Range("D2").Cells(1, 1).Value,
    Len(Range("D2")) - 4))
Range("A3") = (Left(Range("A2").Cells(1, 1).Value,
    Len(Range("A2")) - 29))
Range("A3") = (Right(Range("A3").Cells(1, 1).Value,
    Len(Range("A3")) - 14))
Range("A3") = Replace(Range("A3").Cells(1, 1).Value, "_",
    "/", , 2)
Range("A3") = Replace(Range("A3").Cells(1, 1).Value, "_", "
", , 1)
Range("A3") = Replace(Range("A3").Cells(1, 1).Value, "_",
    ":", , 2)
Range("A3").Select
Selection.NumberFormat = "0.00"

StartTime = Range("A3")
ActiveSheet.Next.Select
StartCell = 1
StopCell = 1
'*****
*****

'Prepare Times
TimeFormula = "=M2+1/3600/24/" & PointsPerSecond
Worksheets(TestSpecificationName).Range("M2").Cells(1,
    1).Value = StartTime
Worksheets(TestSpecificationName).Range("M3").Cells(1,
    1).Value = TimeFormula
Range("M3").Select
Selection.AutoFill Destination:=Range(Cells(3, 13),
    Cells(FileLength, 13)), Type:=xlFillDefault

'Insert Event Detection Formula & Accidental Trigger
    Prevention
Worksheets(TestSpecificationName).Range(Cells(FileLength +
    1, 2), Cells(FileLength + 1 + IgnoreTime, 9)).Value =
    -999
ActualCell = 2 + CompareTime

'Start Formula
Worksheets(TestSpecificationName).Range("S1").Cells(ActualC
    ell, 1).Value = "=MIN(B2:B" & ActualCell & ")"
Range("S1").Cells(ActualCell, 1).Select

```



```

Selection.AutoFill Destination:=Range (Cells (ActualCell,
    19), Cells (ActualCell, 26)), Type:=xlFillDefault
Range (Cells (ActualCell, 19), Cells (ActualCell, 26)).Select
Selection.AutoFill Destination:=Range (Cells (ActualCell,
    19), Cells (FileLength, 26)), Type:=xlFillDefault

Worksheets (TestSpecificationName).Range ("AB1").Cells (Actual
    Cell, 1).Value = "=B" & ActualCell & "-S" &
    ActualCell
Range ("AB1").Cells (ActualCell, 1).Select
Selection.AutoFill Destination:=Range (Cells (ActualCell,
    28), Cells (ActualCell, 35)), Type:=xlFillDefault
Range (Cells (ActualCell, 28), Cells (ActualCell, 35)).Select
Selection.AutoFill Destination:=Range (Cells (ActualCell,
    28), Cells (FileLength, 35)), Type:=xlFillDefault

Worksheets (TestSpecificationName).Range ("Q1").Cells (ActualC
    ell, 1).Value = "=IF (OR (AB" & ActualCell & ">" &
    Threshold & ",AC" & ActualCell & ">" & Threshold &
    ",AD" & ActualCell & ">" & Threshold & ",AE" &
    ActualCell & ">" & Threshold & ",AF" & ActualCell &
    ">" & Threshold & ",AG" & ActualCell & ">" &
    Threshold & ",AH" & ActualCell & ">" & Threshold &
    ",AI" & ActualCell & ">" & Threshold & "),1,0)"
Worksheets (TestSpecificationName).Range ("K1").Cells (ActualC
    ell, 1).Value = "=IF (AND (Q" & ActualCell & "=1,SUM (Q"
    & ActualCell - IgnoreTime & ":Q" & ActualCell &
    ")=1),1,0)"

Range ("Q1").Cells (ActualCell, 1).Select
Selection.AutoFill Destination:=Range (Cells (ActualCell,
    17), Cells (FileLength, 17)), Type:=xlFillDefault
Range ("K1").Cells (ActualCell, 1).Select
Selection.AutoFill Destination:=Range (Cells (ActualCell,
    11), Cells (FileLength, 11)), Type:=xlFillDefault

Range ("K1").Cells (1 + CompareTime, 1).Value = "Start
    Triggers (Filtered)"
Range ("L1").Cells (1 + CompareTime, 1).Value = "Stop
    Trigger"
Range ("Q1").Cells (1 + CompareTime, 1).Value = "All Start
    Triggers"
Range ("R1").Cells (1 + CompareTime, 1).Value = "
    Minimums"
Range ("AB1").Cells (1 + CompareTime, 1).Value =
    "Differences"

'Stop Formula
Worksheets (TestSpecificationName).Range ("L1").Cells (ActualC
    ell, 1).Value = "=IF (OR (B2-B" & 2 + CompareTime & ">"
    & Threshold - 0.25 & ",C2-C" & 2 + CompareTime & ">"
    & Threshold - 0.25 & ",D2-D" & 2 + CompareTime & ">"
    & Threshold - 0.25 & ",E2-E" & 2 + CompareTime & ">"
    & Threshold - 0.25 & ",F2-F" & 2 + CompareTime & ">"
    & Threshold - 0.25 & ",G2-G" & 2 + CompareTime & ">"

```



```

        & Threshold - 0.25 & ",H2-H" & 2 + CompareTime & ">"
        & Threshold - 0.25 & ",I2-I" & 2 + CompareTime & ">"
        & Threshold - 0.25 & ")," , -1, 0) "
Worksheets(TestSpecificationName).Range("L1").Cells(ActualCell, 1).Select
Selection.AutoFill Destination:=Range(Cells(ActualCell, 12), Cells(FileLength, 12)), Type:=xlFillDefault
Worksheets(TestSpecificationName).Range("A1").Cells(FileLength, 12).Value = -1

Worksheets(TestSpecificationName).Range("N1").Cells(1, 1).Value = "# Events"
Worksheets(TestSpecificationName).Range("N2").Cells(1, 1).Value = "=SUM(K:K)-N5"
Worksheets(TestSpecificationName).Range("N4").Cells(1, 1).Value = "# Duplicate Triggers"
Calculate

NumberEvents =
    Worksheets(TestSpecificationName).Range("N2").Cells(1, 1).Value
'MsgBox ("Initial Calculations Complete for File " & FNum & ". " & vbCrLf & "Approximately " & NumberEvents & " Events Found.")

'Finalize Times
Range(Cells(2, 1), Cells(FileLength, 1)) = Range(Cells(2, 13), Cells(FileLength, 13)).Value
Range(Cells(2, 13), Cells(FileLength, 13)).Clear

'Find an Event Start
Range("K1").Cells(StartCell, 1).Select
Columns("K:K").Select
Columns("K:K").Find(What:="1", After:=ActiveCell, LookIn:=xlValues, LookAt:=xlPart, SearchOrder:=xlByRows, SearchDirection:=xlNext, MatchCase:=False, SearchFormat:=False).Activate
StartCell = ActiveCell.Row
Range("L1").Cells(StartCell, 1).Select
'Columns("L:L").Select

Repeat:
Columns("L:L").Find(What:="-1", After:=ActiveCell, LookIn:=xlValues, LookAt:=xlPart, SearchOrder:=xlByRows, SearchDirection:=xlNext, MatchCase:=False, SearchFormat:=False).Activate
StopCell = ActiveCell.Row
If StopCell < StartCell Then GoTo Repeat

FakeEventCounter = 0
FirstEvent = StartCell
EventRow = StartCell
BaseValue1978 = Cells(StartCell - CompareTime, 2).Value
If TimeofYear = "Summer" Then
    BaseValue1985 = Cells(StartCell - CompareTime, 6).Value
Else

```



```

        BaseValue1985 = Cells(StartCell - CompareTime,
            8).Value
    End If
    BaseValue1988 = Cells(StartCell - CompareTime, 9).Value
    mybook.Sheets(TestSpecificationName).Activate

    'Copy Event Data into New Files
    Do
        'Copy Event Data
        MyRange = 0
        If StopCell - StartCell + BeforeEventTime <
            MaxStallTime Then
            MyRange = Range(Cells(StartCell -
                BeforeEventTime, 1), Cells(StopCell
                + AfterEventTime, 9))
            MinValueRange = Range(Cells(StartCell,
                19), Cells(StartCell, 26))
        Else
            MyRange = Range(Cells(StartCell -
                BeforeEventTime, 1),
                Cells(StartCell + MaxStallTime -
                BeforeEventTime, 9))
            MinValueRange = Range(Cells(StartCell,
                19), Cells(StartCell, 26))
        End If

        'Create & Set Up New Workbook
        Set BaseWks =
            Workbooks.Add(xlWBATWorksheet).Worksheets
            (1)
        Worksheets("Sheet1").Range("A1").Cells(1,
            1).Value = "Time"
        Worksheets("Sheet1").Range("A1").Cells(1,
            2).Value = "B1978"
        Worksheets("Sheet1").Range("A1").Cells(1,
            3).Value = "B1979"
        Worksheets("Sheet1").Range("A1").Cells(1,
            4).Value = "B1980"
        Worksheets("Sheet1").Range("A1").Cells(1,
            5).Value = "B1984"
        Worksheets("Sheet1").Range("A1").Cells(1,
            6).Value = "B1985"
        Worksheets("Sheet1").Range("A1").Cells(1,
            7).Value = "B1986"
        Worksheets("Sheet1").Range("A1").Cells(1,
            8).Value = "B1987"
        Worksheets("Sheet1").Range("A1").Cells(1,
            9).Value = "B1988"
        Worksheets("Sheet1").Range(Cells(1, 1),
            Cells(1, 9)).Font.Bold = True
        Worksheets("Sheet1").Range("K1").Cells(1,
            1).Value = "Mins:"
        Worksheets("Sheet1").Range("K2").Cells(1,
            1).Value = "=B2-K$1"
        Worksheets("Sheet1").Range(Cells(1, 11),
            Cells(1, 18)).Font.Italic = True
    
```



```

Worksheets("Sheet1").Range("K1").Cells(1,
    1).HorizontalAlignment = xlRight

'Paste Data Into New Workbook
If StopCell - StartCell < MaxStallTime Then
    BaseWks.Range(Cells(2, 1), Cells(StopCell
        - StartCell + BeforeEventTime +
        AfterEventTime + 1, 9)).Select
    BaseWks.Range(Cells(2, 1), Cells(StopCell
        - StartCell + BeforeEventTime +
        AfterEventTime + 1, 9)).Value =
        MyRange
Else
    BaseWks.Range(Cells(2, 1),
        Cells(MaxStallTime + 1, 9)).Select
    BaseWks.Range(Cells(2, 1),
        Cells(MaxStallTime + 1, 9)).Value =
        MyRange
End If
BaseWks.Range(Cells(1, 11), Cells(1, 18)).Value
    = MinValueRange
BaseWks.Range("A1").Cells(BeforeEventTime + 2,
    1).NumberFormat = "mm/dd/yyyy
    hh:mm:ss.ss;@"
If Filename =
    Replace(Replace(CStr(BaseWks.Range("A1").
        Cells(BeforeEventTime + 2, 1)), "/", "-
    "), ":", ";") Then
    Filename =
        Replace(Replace(CStr(BaseWks.Range(
            "A1").Cells(BeforeEventTime + 2,
            1)), "/", "-"), ":", ";") & " (2)"
Else
    Filename =
        Replace(Replace(CStr(BaseWks.Range(
            "A1").Cells(BeforeEventTime + 2,
            1)), "/", "-"), ":", ";")
End If

'Save And Exit
BaseWks.SaveAs Filename:=EventDataPath &
    Filename, FileFormat:=xlOpenXMLWorkbook
BaseWks.Activate
ActiveWorkbook.Close savechanges:=False

0:      'Next Workbook
        mybook.Sheets(TestSpecificationName).Activate
        Range("K1").Cells(StartCell, 1).Select
        Columns("K:K").Find(What:="1",
            After:=ActiveCell, LookIn:=xlValues,
            LookAt:=xlPart, SearchOrder:=xlByRows,
            SearchDirection:=xlNext,
            MatchCase:=False,
            SearchFormat:=False).Activate
        StartCell = ActiveCell.Row
        If StartCell - EventRow <= PointsPerSecond * 10
            And StartCell - EventRow > -1000 Then

```



```

ComparisonValue1978 = Cells(StartCell,
    2).Value
If TimeofYear = "Summer" Then
    ComparisonValue1985 =
        Cells(StartCell, 6).Value
Else
    ComparisonValue1985 =
        Cells(StartCell, 8).Value
End If
ComparisonValue1988 = Cells(StartCell,
    9).Value
BaseValue1978 = Cells(StartCell, 2).Value
If TimeofYear = "Summer" Then
    BaseValue1985 = Cells(StartCell, 6
        + 17).Value
Else
    BaseValue1985 = Cells(StartCell, 8
        + 17).Value
End If
BaseValue1985 = Cells(StartCell, 9 +
    17).Value

If ComparisonValue1978 - BaseValue1978 >
    Threshold * 1.6 Or
    ComparisonValue1985 - BaseValue1985
    > Threshold * 1.6 Then 'Megaevent
    Protection
    FakeEventCounter = FakeEventCounter
        + 1
    GoTo 0
ElseIf ComparisonValue1978 -
    BaseValue1978 + 0.2 <
    ComparisonValue1988 -
    BaseValue1988 And
    ComparisonValue1985 -
    BaseValue1985 + 0.2 <
    ComparisonValue1988 -
    BaseValue1988 Then 'Sidewalk
    Sensor
    FakeEventCounter = FakeEventCounter
        + 1
    GoTo 0
'ElseIf
    WorksheetFunction.Max(Cells(EventRo
    w, 2).Value, ComparisonValue1978) -
    WorksheetFunction.Min(Range(Cells(E
    ventRow, 2), Cells(StartCell, 2)))
    < 0.5 And
    WorksheetFunction.Max(Cells(EventRo
    w, 7).Value, ComparisonValue1985) -
    WorksheetFunction.Min(Range(Cells(E
    ventRow, 7), Cells(StartCell, 7)))
    < 0.5 Then 'Prevents the tail
    end of the event being classified
    as an event
    'FakeEventCounter =
        FakeEventCounter + 1

```



```

        'GoTo 0
    End If
End If
Range("L1").Cells(StartCell, 1).Select
Columns("L:L").Find(What:="-1",
    After:=ActiveCell, LookIn:=xlValues,
    LookAt:=xlPart, SearchOrder:=xlByRows,
    SearchDirection:=xlNext,
    MatchCase:=False,
    SearchFormat:=False).Activate
StopCell = ActiveCell.Row
EventRow = StartCell
If EventRow > 73000 Then
    qwerty = 1
End If

Loop Until EventRow = FirstEvent

' Save & Close TDMS File
Range("A2").NumberFormat = "mm/dd/yyyy hh:mm:ss;@"
Worksheets(TestSpecificationName).Range("N5").Cells(1,
    1).Value = FakeEventCounter
Filename = Replace(Replace(CStr(Range("A2")), "/", "-"),
    ":", ";")
mybook.SaveAs Filename:=EventDataPath & "Normal Recording
    File " & Filename, FileFormat:=xlOpenXMLWorkbook
mybook.Close savechanges:=False

' Open The Next Normal Recording File.
Next FNum
End If

' Restore the application properties.
With Application
    .ScreenUpdating = True
    .EnableEvents = True
    .Calculation = xlAutomatic
    .CalculateBeforeSave = True
End With
MsgBox "Events Have Been Extracted."

End Sub

```


Strain Compilation VBA Program

```
Sub Compile_Maximum_Event_Strains()
    Dim MyPath As String, FilesInPath As String
    Dim MyFiles() As String
    Dim FNum As Long
    Dim mybook As Workbook, BaseWks As Worksheet
    Dim CalcMode As Long
    Dim MyDate As String

'*****
'*****

    MyPath = Worksheets("Main").Range("D16").Cells(1, 1).Value
    PointsPerSecond = Worksheets("Main").Range("D23").Cells(1, 1).Value
    BeforeTime = Worksheets("Main").Range("D24").Cells(1, 1).Value

'*****
'*****

    BeforeTime = BeforeTime * PointsPerSecond

    ' Add a slash after MyPath if needed.
    If Right(MyPath, 1) <> "\" Then
        MyPath = MyPath & "\"
    End If

    ' If there are no xlsx files in the folder, stop program.
    FilesInPath = Dir(MyPath & "*.xlsx")
    If FilesInPath = "" Then
        MsgBox "No xlsx files found"
        Exit Sub
    End If

    ' Fill the myFiles array with the list of Excel files in the folder.
    FNum = 0
    Do While FilesInPath <> ""
        FNum = FNum + 1
        ReDim Preserve MyFiles(1 To FNum)
        MyFiles(FNum) = FilesInPath
        FilesInPath = Dir()
    Loop

    xsx = LBound(MyFiles)
    yxy = UBound(MyFiles)

    ' Change application properties.
    With Application
        CalcMode = .Calculation
        .Calculation = xlCalculationManual
        .ScreenUpdating = False
        .EnableEvents = False
    End With

    ' Add a new workbook with one sheet; set up headers.
    Set BaseWks = Workbooks.Add(xlWBATWorksheet).Worksheets(1)
    Worksheets("Sheet1").Range("A1").Cells(1, 1).Value = "Time of Trigger
        (i.e. when the first sensor hits 2 µe)"
    Worksheets("Sheet1").Range("A1").Cells(1, 2).Value = "B1978"
```



```

Worksheets("Sheet1").Range("A1").Cells(1, 3).Value = "B1979"
Worksheets("Sheet1").Range("A1").Cells(1, 4).Value = "B1980"
Worksheets("Sheet1").Range("A1").Cells(1, 5).Value = "B1984"
Worksheets("Sheet1").Range("A1").Cells(1, 6).Value = "B1985"
Worksheets("Sheet1").Range("A1").Cells(1, 7).Value = "B1986"
Worksheets("Sheet1").Range("A1").Cells(1, 8).Value = "B1987"
Worksheets("Sheet1").Range("A1").Cells(1, 9).Value = "B1988"
Worksheets("Sheet1").Range("A1").Cells(1, 11).Value = "Drift"
'Worksheets("Sheet1").Range("A1").Cells(1, 13).Value = 0
'Worksheets("Sheet1").Range("A1").Cells(1, 14).Value = 2
'Worksheets("Sheet1").Range("A1").Cells(1, 15).Value = 4
'Worksheets("Sheet1").Range("A1").Cells(1, 16).Value = 6
'Worksheets("Sheet1").Range("A1").Cells(1, 17).Value = 8
'Worksheets("Sheet1").Range("A1").Cells(1, 18).Value = 10
'Worksheets("Sheet1").Range("A1").Cells(1, 19).Value = 12
'Worksheets("Sheet1").Range("A1").Cells(1, 20).Value = 14
'Worksheets("Sheet1").Range("A1").Cells(1, 21).Value = 16
'Worksheets("Sheet1").Range("A1").Cells(1, 22).Value = 18
'Worksheets("Sheet1").Range("A1").Cells(1, 23).Value = 20
'Worksheets("Sheet1").Range("A1").Cells(1, 24).Value = "Infinity"

Worksheets("Sheet1").Range(Cells(1, 1), Cells(1, 24)).Font.Bold = True
BaseWks.SaveAs fileName:="C:\Users\jake\Desktop\Master File",
    FileFormat:=xlOpenXMLWorkbook

' Loop through all files in the myFiles array.
If FNum > 0 Then
    For FNum = LBound(MyFiles) To UBound(MyFiles)
        Set mybook = Nothing
        On Error Resume Next
        Set mybook = Workbooks.Open(MyPath & MyFiles(FNum))
        On Error GoTo 0

        'Select Correct Sheet & Copy Data Out
        MyDate = Range("A1").Cells(2 + BeforeTime, 1)
        Value1 = WorksheetFunction.Max(Range(Cells(2 +
            BeforeTime, 2), Cells(450, 2))) - Range("K1")
        Value2 = WorksheetFunction.Max(Range(Cells(2 +
            BeforeTime, 3), Cells(450, 3))) - Range("L1")
        Value3 = WorksheetFunction.Max(Range(Cells(2 +
            BeforeTime, 4), Cells(450, 4))) - Range("M1")
        Value4 = WorksheetFunction.Max(Range(Cells(2 +
            BeforeTime, 5), Cells(450, 5))) - Range("N1")
        Value5 = WorksheetFunction.Max(Range(Cells(2 +
            BeforeTime, 6), Cells(450, 6))) - Range("O1")
        Value6 = WorksheetFunction.Max(Range(Cells(2 +
            BeforeTime, 7), Cells(450, 7))) - Range("P1")
        Value7 = WorksheetFunction.Max(Range(Cells(2 +
            BeforeTime, 8), Cells(450, 8))) - Range("Q1")
        Value8 = WorksheetFunction.Max(Range(Cells(2 +
            BeforeTime, 9), Cells(450, 9))) - Range("R1")

        'Paste Data into Master Sheet
        Windows("Master File").Activate
        Worksheets("Sheet1").Range("A2").Cells(FNum, 1).Value =
            MyDate
    
```



```

Worksheets("Sheet1").Range("A2").Cells(FNum, 2).Value =
    Value1
Worksheets("Sheet1").Range("A2").Cells(FNum, 3).Value =
    Value2
Worksheets("Sheet1").Range("A2").Cells(FNum, 4).Value =
    Value3
Worksheets("Sheet1").Range("A2").Cells(FNum, 5).Value =
    Value4
Worksheets("Sheet1").Range("A2").Cells(FNum, 6).Value =
    Value5
Worksheets("Sheet1").Range("A2").Cells(FNum, 7).Value =
    Value6
Worksheets("Sheet1").Range("A2").Cells(FNum, 8).Value =
    Value7
Worksheets("Sheet1").Range("A2").Cells(FNum, 9).Value =
    Value8

' Close TDMS File
mybook.Close savechanges:=False

' Open the next workbook.
Next FNum
End If

'Drift Column
Worksheets("Sheet1").Range("K2").Cells(1, 1).Value =
    "=IF(AND(B2<2,C2<2,D2<2,E2<2,F2<2,G2<2,H2<2,I2<2),1,0)"
Range("K2").Select
Selection.AutoFill Destination:=Range(Cells(2, 11), Cells(FNum, 11)),
    Type:=xlFillDefault

'Create tally table
'Worksheets("Sheet1").Range("N2").Cells(1, 1).Value =
    "=IF(AND($B2>=M$1,$B2<N$1,$K2<>1),1,0)"
'Range("N2").Select
'Selection.AutoFill Destination:=Range("N2:X2"), Type:=xlFillDefault
'Range("N2:X2").Select
'Selection.AutoFill Destination:=Range(Cells(2, 14), Cells(FNum, 24)),
    Type:=xlFillDefault
'Worksheets("Sheet1").Range("A1").Cells(1, 26).Value = "0-2"
'Worksheets("Sheet1").Range("A1").Cells(1, 27).Value = "2-4"
'Worksheets("Sheet1").Range("A1").Cells(1, 28).Value = "4-6"
'Worksheets("Sheet1").Range("A1").Cells(1, 29).Value = "6-8"
'Worksheets("Sheet1").Range("A1").Cells(1, 30).Value = "8-10"
'Worksheets("Sheet1").Range("A1").Cells(1, 31).Value = "10-12"
'Worksheets("Sheet1").Range("A1").Cells(1, 32).Value = "12-14"
'Worksheets("Sheet1").Range("A1").Cells(1, 33).Value = "14-16"
'Worksheets("Sheet1").Range("A1").Cells(1, 34).Value = "16-18"
'Worksheets("Sheet1").Range("A1").Cells(1, 35).Value = "18-20"
'Worksheets("Sheet1").Range("A1").Cells(1, 36).Value = "20+"
'Worksheets("Sheet1").Range("A1").Cells(1, 37).Value = "Sum:"
Worksheets("Sheet1").Range("A1").Cells(1, 39).Value = "# of Drifts"
'Worksheets("Sheet1").Range("A1").Cells(2, 26).Value = "=SUM(N:N)-N1"
'Worksheets("Sheet1").Range("A1").Cells(2, 27).Value = "=SUM(O:O)-O1"
'Worksheets("Sheet1").Range("A1").Cells(2, 28).Value = "=SUM(P:P)-P1"
'Worksheets("Sheet1").Range("A1").Cells(2, 29).Value = "=SUM(Q:Q)-Q1"

```



```

Worksheets("Sheet1").Range("A1").Cells(2, 30).Value = "=SUM(R:R)-R1"
Worksheets("Sheet1").Range("A1").Cells(2, 31).Value = "=SUM(S:S)-S1"
Worksheets("Sheet1").Range("A1").Cells(2, 32).Value = "=SUM(T:T)-T1"
Worksheets("Sheet1").Range("A1").Cells(2, 33).Value = "=SUM(U:U)-U1"
Worksheets("Sheet1").Range("A1").Cells(2, 34).Value = "=SUM(V:V)-V1"
Worksheets("Sheet1").Range("A1").Cells(2, 35).Value = "=SUM(W:W)-W1"
Worksheets("Sheet1").Range("A1").Cells(2, 36).Value = "=SUM(X:X)"
Worksheets("Sheet1").Range("A1").Cells(2, 37).Value = "=SUM(Z2:AJ2)"
Worksheets("Sheet1").Range("A1").Cells(2, 39).Value = "=SUM(K:K)"
Worksheets("Sheet1").Range(Cells(1, 26), Cells(1, 39)).Font.Bold = True
Worksheets("Sheet1").Range("Y5").Cells(1, 1).Value = "'<-Values set up
    for Sensor B1978"

' Restore the application properties.
With Application
    .ScreenUpdating = True
    .EnableEvents = True
    .Calculation = xlAutomatic
End With

'Freeze Header Row/Timestamp Column
Range("B2").Select
ActiveWindow.FreezePanels = True

'Clean up time data
'Columns("A:A").Select
'Selection.Replace What:="-", Replacement:="/", LookAt _
    :=xlPart, SearchOrder:=xlByRows, MatchCase:=False,
    SearchFormat:=False, _
    ReplaceFormat:=False
'Selection.Replace What:=".", Replacement:=":", LookAt _
    :=xlPart, SearchOrder:=xlByRows, MatchCase:=False,
    SearchFormat:=False, _
    ReplaceFormat:=False
'Range("A1").Select

'Set the column width in the new workbook.
Windows("Master File").Activate
ActiveWorkbook.Save
BaseWks.Columns.AutoFit
Columns("A:A").ColumnWidth = 25
Columns("A:A").HorizontalAlignment = xlLeft
Columns("Y:Y").ColumnWidth = 8.43
MsgBox "Data Extraction Complete."
Worksheets("Sheet1").Range(Cells(2, 1), Cells(FNum, 1)).NumberFormat =
    "m/d/yyyy h:mm:ss AM/PM"

End Sub

```